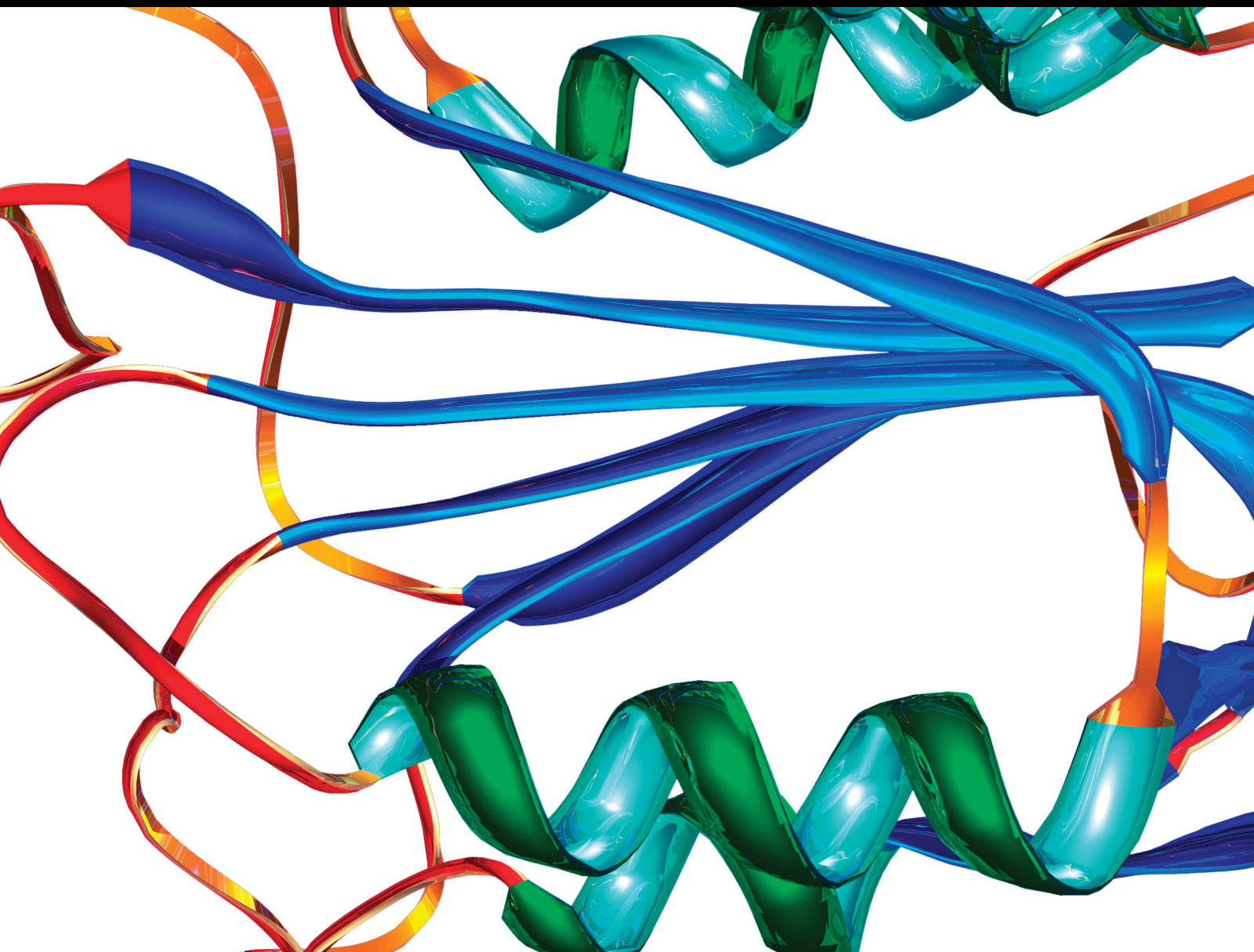# Biomarkers in Acute Lung Injury Induced by Surgical Critical Care Conditions

Lead Guest Editor: Jing Huirong
Guest Editors: Zhe Fan, QiXing Chen, Dapeng Chen, and Jens-Christian Schewe

Biomarkers in Acute Lung Injury Induced by Surgical Critical Care Conditions

Biomarkers in Acute Lung Injury Induced by Surgical Critical Care Conditions

Lead Guest Editor: Jing Huirong
Guest Editors: Zhe Fan, QiXing Chen, Dapeng Chen, and Jens-Christian Schewe

Alexander G. Mathioudakis, United Kingdom
Andrea Maugeri, Italy
Prasenjit Mitra, India
Ekansh Mittal, USA
Hiroshi Miyamoto, USA
Naoshad Muhammad, USA
Chiara Nicolazzo, Italy
Xing Niu, China
Dong Pan, USA
Dr.Krupakar Parthasarathy, India
Robert Pichler, Austria
Dimitri Poddighe, Kazakhstan
Roberta Rizzo, Italy
Maddalena Ruggieri, Italy
Tamal Sadhukhan, USA
Pier P. Sainaghi, Italy
Cristian Scheau, Romania
Jens-Christian Schewe, Germany
Alexandra Scholze, Denmark
Shabana, Pakistan
Anja Hviid Simonsen, Denmark
Eric A. Singer, USA
Daniele Sola, Italy
Timo Sorsa, Finland
Yaying Sun, China
Mohammad Tarique, USA
Jayaraman Tharmalingam, USA
Sowjanya Thatikonda, USA
Stamatios E. Theocharis, Greece
Tilman Todenhöfer, Germany
Anil Tomar, India
Alok Tripathi, India
Drenka Trivanović, Germany
Natacha Turck, Switzerland
Azizah Ugusman, Malaysia
Shailendra K. Verma, USA
Aristidis S. Veskoukis, Greece
Arianna Vignini, Italy
Jincheng Wang, Japan
Zhongqiu Xie, USA
Yuzhen Xu, China
Zhijie Xu, China
Guan-Jun Yang, China
Yan Yang, USA

Chengwu Zeng, China
Jun Zhang Zhang, USA
Qun Zhang, China
Changli Zhou, USA
Heng Zhou, China
Jian-Guo Zhou, China

Contents

Review Article

Signal Pathways and Markers Involved in Acute Lung Injury Induced by Acute Pancreatitis

Jialin Zhou,[1] Pengcheng Zhou,[2] Yingyi Zhang [ID],[1] Guangzhi Wang [ID],[3] and Zhe Fan [ID][1,2]

[1]*Department of General Surgery, The Third People's Hospital of Dalian, Dalian Medical University, Dalian, China*
[2]*School of Medicine, Southeast University, Nanjing, China*
[3]*Department of General Surgery, The Second Hospital of Dalian Medical University, Dalian, China*

Correspondence should be addressed to Guangzhi Wang; wanggz@dmu.edu.cn and Zhe Fan; fanzhe1982@hotmail.com

Acute pancreatitis (AP) is a common acute abdominal disease with a mortality rate of about 30%. Acute lung injury (ALI) is a common systemic complication of acute pancreatitis, with progressive hypoxemia and respiratory distress as the main manifestations, which can develop into acute respiratory distress syndrome or even multiple organ dysfunction syndrome (MODS) in severe cases, endangering human health. In the model of AP, pathophysiological process of the lung can be summarized as oxidative stress injury, inflammatory factor infiltration, and alveolar cell apoptosis. However, the intrinsic mechanisms underlying AP and how it leads to ALI are not fully understood. In this paper, we summarize recent articles related to AP leading to ALI, including the signal transduction pathways and biomarkers of AP-ALI. There are factors or pathway aggravating ALI, the JAK2-STAT3 signaling pathway, NLRP3/NF-κB pathway, mitogen-activated protein kinase, PKC pathway, neutrophil protease (NP)-LAMC2-neutrophil pathway, and the P2X7 pathway, and there are important transcription factors in the NRF2 signal transduction pathway which could give researchers better understanding of the underlying mechanisms controlling AP and ALI and lay the foundation for finally curing ALI induced by AP.

1. Introduction

Acute pancreatitis (AP) is an acute inflammatory process of the pancreas, which can injure not only local peripancreatic tissue but remote organs and systems as well [1]. The acute inflammatory state of the pancreas usually follows an infection, which may lead to multisystem organ dysfunction, including acute lung injury (ALI) [2–4]. During this pathophysiological process, cytokines and inflammatory mediators are released in large quantities, activating multiple signaling pathways which cause damage to the body. However, the underlying mechanism is not completely clear. In recent years, the signaling pathways mediating the occurrence of severe AP (SAP) have become better known, and it has now been shown that multiple signaling pathways are involved in the biological processes of alveolar endothelial cell proliferation, differentiation, and apoptosis caused by AP. In this paper, we summarize the roles of seven pathways and related biomarkers in AP-ALI which have increased our understanding of the development of the disease and provided novel therapeutic approaches for its treatment.

2. JAK2-STAT3 Signaling Pathway

The Janus kinase/signal transducer and activator of transcription (JAK/STAT) pathway has previously been shown to play a role in tumorigenesis. Interleukin-6 (IL-6) is a proinflammatory cytokine that preferentially activates STAT3 and has a role in both initiating and exacerbating the inflammatory process. During inflammation, adhesion molecules, substances expressed on endothelial cells (ECs), contribute to the recruitment and migration of leukocytes to the subendothelial stroma [5].

AP can induce the expression of intercellular adhesion molecule-1 (ICAM-1) through the JAK2/STAT3 signaling pathway, and the induction of ICAM-1 is associated with leukocyte adhesion and migration, leading to amplification of endothelial cell injury and inflammatory response. In
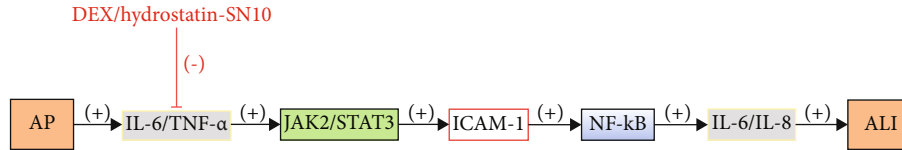
FIGURE 1: AP can activate IL-6 and TNF-α, further activating the JAK2/STAT3 pathway, leading to ICAM-1 activation and promoting the upregulation of NF-κB, which in turn induces the development of ALI. DEX/hydrostatin-SN10 inhibits this pathway.
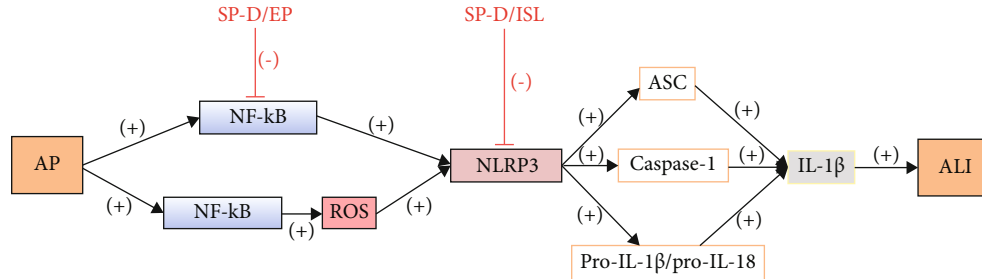
FIGURE 2: AP may cause NF-κB signaling initiation and also NF-κB-mediated activation of ROS produced by inflammation, which leads to activation of NLRP3 and consequent recruitment of ASC, activation of caspase-1, and induction of pro-IL-1β or pro-IL-18 into mature forms, which can then induce the activation of cytokines (e.g., IL-1β) and thereby promote lung injury in ALI. ISL inhibits NLRP3 activation, and EP inhibits NF-κB activation, both of which attenuate severe pancreatitis-associated ALI.

addition, AP can activate IL-6 and tumor necrosis factor (TNF)-α, further activating the JAK2/STAT3 pathway, leading to ICAM-1 activation and promoting the upregulation of nuclear factor-κB (NF-κB), which in turn induces the development of ALI [6].

It has been suggested that high levels of tumor necrosis factor alpha (TNF-α) and nuclear factor-κB (NF-κB) may induce the expression of ICAM-1 and thus be involved in the development of SAP-ALI [6]. Dexamethasone treatment attenuates SAP-induced upregulation of TNF-α and NF-κB [7]. Dexamethasone treatment may reduce cytokine production by inhibiting ICAM-1, which may be a cause of its anti-inflammatory effect [6]. IL-6 inhibits proliferation, promotes apoptosis, and contributes to lung injury by activating the JAK2/STAT3 signaling pathway [8–10]. A short mutant peptide of hydrostatin-SN10 (peptide sequence, DEQHLETELH) extracted from snake venom inhibits AP-ALI by inhibiting IL-6 induced by JAK2/-STAT3 signaling (Figure 1).

3. NLRP3/NF-κB Pathway

Protein 3 (NLRP3) inflammasome is a substance containing NACHT, LRR, and PYD domains that leads to the production of IL-1β and IL-18 by sensing pathogen and danger-related molecular patterns (PAMPs and DAMPs) [11]. NF-κB signaling is an important initial step in initiating NLRP3 activation, and reactive oxygen species (ROS) generated by NF-κB-mediated inflammation are also a risk signal for NLRP3 activation [12]. NLRP3 activation is followed by ASC recruitment, activation of cysteine protease-1 (caspase-1), and induction of pro-IL-1β or pro-IL-18 processing and maturation [13, 14]. Thus, both signals, NLRP3 and NF-κB, act together to induce the activation of cytokines (e.g., IL-1β) that promote ALI.

Lack of functional Toll-like receptor 4 (TLR4) leads to a decreased NF-κB response and reduced production of proinflammatory mediators, ameliorating lung inflammation in mice and alveolar macrophages [15]. In addition, monocyte chemotactic protein-1 (MCP-1) is an important factor that has been shown to induce AP as a direct target of NF-κB [16, 17].

Surfactant protein D (SP-D) inhibits SAP-induced ALI and pancreatic injury. It may do so through a pathway that inhibits the activation of NLRP3, inflammasome, and NF-κB signaling [18]. Isoflavonopoietin (ISL), a flavonoid derived from licorice, can inhibit NLRP3 pathway by activating Nrf2, inhibiting NF-κB, and also inhibiting NLRP3 activation [19, 20]. Ethylpyruvate inhibits NF-κB activation and downregulates downstream inflammatory cytokine expression in SAP rats and attenuates severe pancreatitis-associated ALI [21] (Figure 2).

4. Mitogen-Activated Protein Kinase (MAPK)

Mitogen-activated protein kinase (MAPK), including P38MAPK, c-Jun N-terminal kinase (JNK), and extracellular signal-regulated kinase (ERK), is a member of the serine/-threonine kinase family and plays an important role in inflammation, tumorigenesis, cell proliferation, apoptosis, differentiation, and stress responses [22–25]. ERK is activated in response to ischemic injury, such as hemorrhagic shock and stroke, and its activation may lead to cell damage and death [26]. The p38MAPK is an important signal transduction enzyme that regulates gene transcription and translation by transducing extracellular signals into cells and is primarily involved in the release of inflammatory cytokines/-mediators in the pathogenesis of inflammatory diseases such as ALI and AP [25, 27]. AP-activated TNF-α induces ALI via p-JNK/MAPK and p-ERK/MAPK in the lung, while
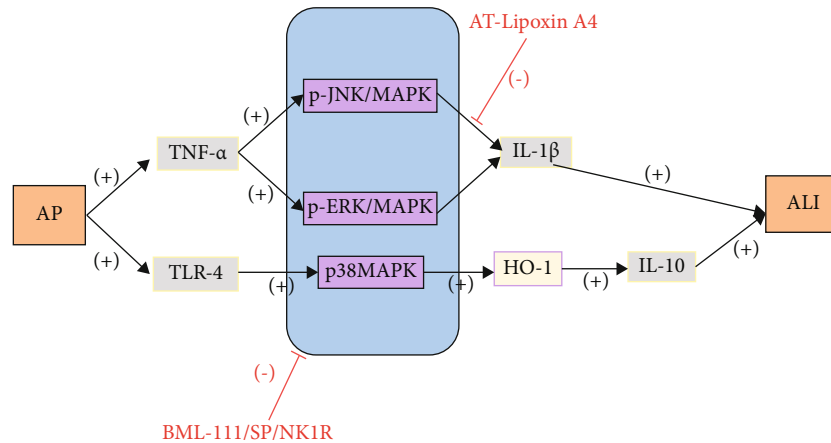
FIGURE 3: AP-activated TNF-α induces ALI via p-JNK/MAPK and p-ERK/MAPK. AP-activated TLR-4 induces ALI via p38MAPK-induced upregulation of HO-1. AT-Lipoxin A4 inhibits the p-JNK/MAPK and p-ERK/MAPK pathways, BML-111 blocks phosphorylation of JNK, ERK, and p38MAPK, and SP/NK1R may prevent ALI by regulating LTB4 production.
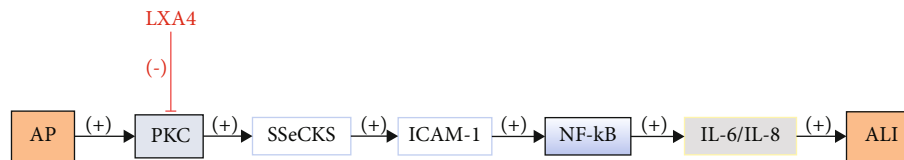
FIGURE 4: AP can cause PKC-mediated upregulation of SSeCKS leading to activation of F-actin and promote upregulation of NF-κB, which in turn induces the development of ALI. LXA4 can inhibit this pathway.

p38MAPK can be activated by a variety of extracellular stimuli, such as inflammatory mediators, heat injury, and ultraviolet light. p38MAPK is activated, and chemokines are increased after hemorrhagic shock and can contribute to the development of ALI [28].

MAPK activation can cause multiorgan dysfunction after hemorrhagic shock (MODS) [29, 30]. Therefore, prevention and control of the MAPK signaling pathway may be an important way to prevent hemorrhagic shock-induced ALI and multiorgan dysfunction. BML-111 blocks phosphorylation of JNK, ERK, and p38MAPK in hemorrhagic shock [31]. AT-Lipoxin A4 inhibits the p-JNK/MAPK and p-ERK/MAPK pathways [32]. Substance P (SP)/neurokinin-1 receptor (NK1R) may regulate pancreatitis leukotriene B4 (LTB4) production via the MAPK signaling pathway, and LTB4 may regulate neutrophil reverse transendothelial migration (rTEM) in AP, which further promotes AP-ALI [32, 33]. Upregulation of microRNA-542-5p downregulates the expression of P21-associated kinase 1 (PAK1), and downregulation of PAK1 may contribute to inhibition of the MAPK signaling pathway [33]. Lipoprotein A4 (LXA4) blocks ALI by inhibiting the inflammatory pathways of NF-κB and p38MAPK and by upregulating cytoprotective heme oxygenase-1 (HO-1) [34] (Figure 3).

5. PKC Pathway

Protein kinase C (PKC) is a member of the family of phospholipid-dependent serine/threonine kinases. It consists of at least several isoforms [35, 36]. Conventional PKC alleles (α, βI, βII, and β), novel PKC isoforms (δ, ε, η, and θ), and other PKC isoforms (λ subclass, γ subclass), as well as four PKC isoforms (α, δ, ε, and ζ), each with a unique activation pattern, have been identified in pancreatic follicular cells [37]. Experimental studies have shown that inflammatory mediators are overproduced and released in the lung through a PKC-dependent pathway [38]. The PKC pathway is an important signaling pathway that can be activated by inflammatory cytokines. src-inhibited C kinase substrate (SSeCKS), a PKC substrate and a major inflammatory response protein that is significantly overexpressed in ALI, selectively binds to signaling proteins such as PKC to disrupt endothelial cell permeability [39]. The PKC pathway regulates cytoskeletal protein activity and endothelial cell barrier function by modulating its downstream substrate SSeCKS. PKC-mediated upregulation of SSeCKS activates F-actin, which leads to NF-κB activation in HPMEC, resulting in ALI [40]. Because rescue of aquaporin 5 (AQP-5) and matrix metalloproteinase 9 (MMP-9) and inhibition of apoptosis may lead to NF-κB attenuation [41], we speculate that NF-κB may be a key mediator of apoptosis, AQP-5/MMP-9, and PKC/SSeCKS/F-actin signaling pathways during AP-induced ALI.

SP regulates LTB4 production via the PKCα/MAPK pathway, which in turn promotes AP-ALI via neutrophil rTEM [42]. LXA4 effectively promotes F-actin remodeling and regulates its expression in pulmonary microvascular endothelial cells both in vivo and in vitro by inhibiting the PKC/SSeCKS signaling pathway [43] (Figure 4).
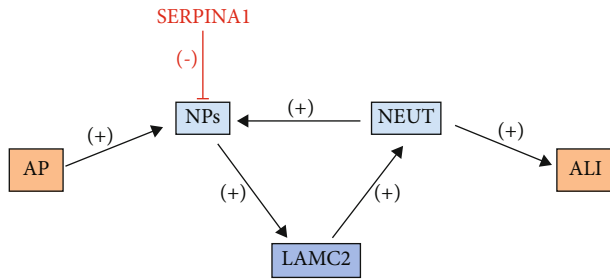
FIGURE 5: Enzymatic cleavage of NPs releases LAMC2 fragments that in turn promote neutrophil recruitment and induce acute phase NP production. LAMC2 has been reported to be overexpressed and associated with ALI in its early stages. It can negatively regulate the activity of NPs to attenuate AP-induced ALI.

6. NPs-LAMC2-Neutrophil Pathway

Laminin gamma 2 (LAMC2) and Serpin Family A Member 1 (SERPINA1) are associated with collagen-containing extracellular matrix, leukocyte-cell adhesion, and regulation of endopeptidases [44]. It has been suggested that the LAMC2 fragment is released by the cleavage of NP enzymes; importantly, the released LAMC2 fragment in turn promotes neutrophil recruitment [45]. This would induce the production of NP in the acute phase. LAMC2 has been reported to be overexpressed and associated with the early stages of ALI. Thus, NPs, LAMC2, and neutrophils may form positive-feedback loops in the pathogenesis of SAP-ALI. Upregulation of LAMC2 expression in SAP-ALI lung tissue may be due to increased expression of LAMC2 in SAP-ALI lung tissue. SERPINA1 is a serine protease inhibitor that negatively regulates the activity of NPs. The high expression level of serine protease inhibitor B1 (serpinB1) in SAP-ALI lung tissue and its possible association with the aggregation of high numbers of neutrophils and monocytes in the lung suggest that it may be a novel biomarker of disease severity. Emodin may exert a protective effect by negatively regulating NP activity and blocking NPs-LAMC2 in SAP-ALI. Neutrophil-altered loops significantly attenuate AP-induced ALI [46] (Figure 5).

7. P2X7 Pathway

SAP is a sterile inflammatory condition characterized by the release of large amounts of proinflammatory cytokines from damaged glandular follicle cells [47]. The purinergic receptor P2X7 is a member of the P2X family of ATP-gated cation channels and an important molecule involved in the inflammatory response [48]. Activation of P2X7 stimulates multiple signaling pathways such as reactive oxygen species (ROS), MAPKs, and NF-κB, which produce large amounts of inflammatory mediators [49, 50]. Recent studies have shown that P2X7 can effectively stimulate inflammatory activation of NLRP3 [51–53]. Numerous studies have shown that P2X7R is mainly expressed in rodent pancreatic ductal cells and regulates calcium signaling and ion transport
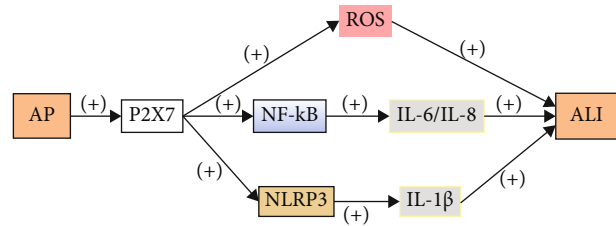
FIGURE 6: AP promotes the activation of P2X7, which stimulates multiple signaling pathways, including ROS, NLRP3, and NF-κB, the latter of which produces large amounts of inflammatory mediators that induce the development of ALI.

[54–56]. Cabili et al. found evidence that NLRP3 receptors are also expressed in the exocrine glands of animals. Alveoli in the pancreas exhibit low functionality and a marked lack of P2X7 receptors for purinergic receptor signaling, but pancreatic duct cells express high amounts of various P2 receptors, especially P2X7 receptors [57]. In addition, SAP is usually initially aseptic, which predisposes to necrosis of the glandular follicle cells [58]. A sterile inflammatory response mediated by damage-associated molecular patterns (DAMP) released from necrotic glandular follicle cells predisposes animals to pancreatic injury, which acts through plasma membrane P2X7 receptors [59]. In addition, the P2X7/NLRP3 pathway is activated 12 h after pancreatic injury. However, inflammation is largely time-course dependent, suggesting that induction of P2X7 is associated with the severity of pancreatitis (Figure 6).

8. NRF2 Signal Transduction Pathway

The nuclear factor erythroid-2-related factor 2 (Nrf2) pathway is thought to be a survival pathway for the mitigation of oxidative damage. Nrf2 is a protective antioxidant that regulates cellular oxidation and reduction homeostasis, and for oxidative stress, the Nrf2 pathway can be modulated to treat SAP [60–62]. Activation of Nrf2 is an important strategy to inhibit ROS generation and control oxidative stress. Furthermore, Nrf2 is an important regulator in ALI [63–65]. Under basal conditions, Nrf2 is present in the cytoplasm as a component of the cell and binds to Kelch-like ECH-associated protein 1 (Keap1), which is ultimately degraded. However, when organisms are under oxidative stress, Nrf2 dissociates from Keap1, a process that can be achieved through various mechanisms such as oxidative modification of cysteine thiols in classical Keap1 and phosphorylation of specific amino acid residues of Nrf2 through multiple protein kinase pathways [66].

The intracellular energy sensor AMP-activated protein kinase (AMPK) is a kinase which is considered to be upstream of Nrf2 and is of interest because of the relationship with redox homeostasis and energy metabolism [67]. In addition, another mechanism of AMPK-mediated Nrf2 activation may include Akt kinase and glycogen synthase kinase 3 beta (GSK3β) [68]. TNF-α can activate the Nrf2 signaling pathway and its downstream gene HO-1; furthermore, LXA4 in HPMEC, as a potent anti-inflammatory
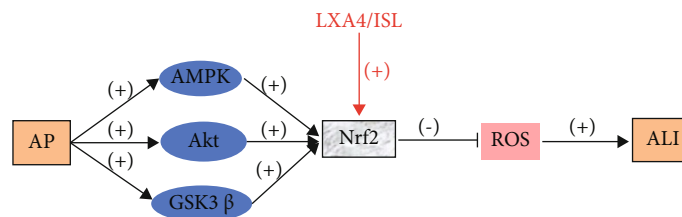
FIGURE 7: AP activates AMPK, which activates Akt kinase and GSK3β to mediate Nrf2 activation. TNF-α activates the Nrf2 signaling pathway and HO-1, and activation of Nrf2 may inhibit ROS production and control oxidative stress, which in turn inhibits ALI. LXA4/ISLT can treat ALI/ARDS by activating Nrf2.

TABLE 1: Indices of ALI induced by acute pancreatitis.

Model	Models induced	Indices of ALI
Mouse	Cerulein [4, 43] L-arginine [33]	Lung tissue W/D ratio [4, 43] MPO activity [33] BALF and cell analysis [4] MDA assays [33] Histological analysis [4, 33, 43]
Rat	Deoxycholic acid sodium salt [6] Sodium taurocholate [21, 31, 46]	Lung tissue W/D ratio [21] MPO activity [21] MDA assays [21] Histological analysis [21, 31, 46]

MPO: myeloperoxidase; MDA: malondialdehyde; W/D ratio: wet/dry weight ratio; BALF: bronchoalveolar lavage fluid.

and novel antioxidant mediator, can further promote Nrf2 expression. LXA4 may attenuate AP-induced inflammation and ROS by regulating the Nrf2 pathway. When injected intraperitoneally, isoliquiritigenin, with a chalcone structure (4,20,40-trihydroxy chalcone), can treat ALI/Acute Respiratory Distress Syndrome (ARDS) associated with gram-negative bacterial infections by activating Nrf2 [69] (Figure 7).

9. Summary and Outlook

AP leads to the continuous activation of various signaling pathways in ALI, as shown in recent studies; ALI was assessed as shown in the indices listed in Table 1. By inhibiting the transduction of the aggravated AP-ALI pathway and promoting the transduction of the attenuated AP-ALI pathway, the secretion of proinflammatory factors can be reduced, pulmonary edema can be reduced, and certain therapeutic effects can be achieved. The discovery of precise and effective target inhibitors still depends on the study of genes and proteins involved in the pathway, but the study of diagnostic genes and proteomics of inflammatory diseases is still at a preliminary stage. Therefore, ALI induced by more surgical critical care conditions needs to be more thoroughly explored, especially in ischemia/reperfusion [70, 71], sepsis [72], trauma [73], and transfusion [74, 75]. In the future, we plan to analyze the interaction between various proteins and genes to deepen our understanding of the mechanism of inflammatory diseases and provide for effective diagnosis and treatments.

Data Availability

The data used to support the findings of this study are available from the corresponding author upon request.

Conflicts of Interest

The authors declare that they have no competing interests.

Authors' Contributions

Jialin Zhou and Pengcheng Zhou contributed equally to this work.

Acknowledgments

References

[1] K. Ito, Y. Igarashi, T. Mimura et al., "Severe acute pancreatitis with complicating colonic fistula successfully closed using the over-the-scope clip system," *Case reports in gastroenterology*, vol. 7, no. 2, pp. 314–321, 2013.

[2] H. Lei, W. Minghao, Y. Xiaonan, X. Ping, L. Ziqi, and X. Qing, "Acute lung injury in patients with severe acute pancreatitis," *The Turkish journal of gastroenterology: the official journal of Turkish Society of Gastroenterology*, vol. 24, no. 6, pp. 502–507, 2013.

[3] G. Lippi, M. Valentino, and G. Cervellin, "Laboratory diagnosis of acute pancreatitis: in search of the Holy Grail," *Critical reviews in clinical laboratory sciences*, vol. 49, no. 1, pp. 18–31, 2012.

[4] N. Matsuda, J. Nishihira, Y. Takahashi, O. Kemmotsu, and Y. Hattori, "Role of macrophage migration inhibitory factor in acute lung injury in mice with acute pancreatitis complicated by endotoxemia," *American journal of respiratory cell and molecular biology*, vol. 35, no. 2, pp. 198–205, 2006.

[5] P. K. Chatterjee, Y. Al-Abed, B. Sherry, and C. N. Metz, "Cholinergic agonists regulate JAK2/STAT3 signaling to suppress endothelial cell activation," *American journal of physiology Cell physiology*, vol. 297, no. 5, pp. C1294–C1306, 2009.

[6] X. Han, Y. Wang, H. Chen et al., "Enhancement of ICAM-1 via the JAK2/STAT3 signaling pathway in a rat model of severe acute pancreatitis-associated lung injury," *Experimental and therapeutic medicine*, vol. 11, no. 3, pp. 788–796, 2016.

[7] L. Ramudo, S. Yubero, M. A. Manso, J. Sanchez-Recio, E. Weruaga, and I. De Dios, "Effects of dexamethasone on intercellular adhesion molecule 1 expression and inflammatory response in necrotizing acute pancreatitis in rats," *Pancreas*, vol. 39, no. 7, pp. 1057–1063, 2010.

[8] J. M. Shieh, H. Y. Tseng, F. Jung, S. H. Yang, and J. C. Lin, "Elevation of IL-6 and IL-33 levels in serum associated with lung fibrosis and skeletal muscle wasting in a bleomycin-induced lung injury mouse model," *Mediators of Inflammation*, vol. 2019, Article ID 7947596, 12 pages, 2019.

[9] F. Ning, H. Zheng, H. Tian et al., "Research on effect of adiponectin on sepsis-induced lung injury in rats through IL-6/STAT3 signaling pathway," *Panminerva medica*, vol. 62, no. 3, pp. 184–186, 2020.

[10] X. Y. Wu, F. Tian, M. H. Su et al., "BF211, a derivative of bufalin, enhances the cytocidal effects in multiple myeloma cells by inhibiting the IL-6/JAK2/STAT3 pathway," *International Immunopharmacology*, vol. 64, pp. 24–32, 2018.

[11] Y. K. Kim, J. S. Shin, and M. H. Nahm, "NOD-like receptors in infection, immunity, and diseases," *Yonsei medical journal*, vol. 57, no. 1, pp. 5–14, 2016.

[12] F. G. Bauernfeind, G. Horvath, A. Stutz et al., "Cutting edge: NF-kappaB activating pattern recognition and cytokine receptors license NLRP3 inflammasome activation by regulating NLRP3 expression," *Journal of immunology*, vol. 183, no. 2, pp. 787–791, 2009.

[13] D. E. Place and T. D. Kanneganti, "Recent advances in inflammasome biology," *Current opinion in immunology*, vol. 50, pp. 32–38, 2018.

[14] A. Abderrazak, T. Syrovets, D. Couchie et al., "NLRP3 inflammasome: from a danger signal sensor to a regulatory node of oxidative stress and inflammatory diseases," *Redox biology*, vol. 4, pp. 296–307, 2015.

[15] E. H. Joh, W. Gu, and D. H. Kim, "Echinocystic acid ameliorates lung inflammation in mice and alveolar macrophages by inhibiting the binding of LPS to TLR4 in NF-κB and MAPK pathways," *Biochemical Pharmacology*, vol. 84, no. 3, pp. 331–340, 2012.

[16] G. X. Zhou, X. J. Zhu, X. L. Ding et al., "Protective effects of MCP-1 inhibitor on a rat model of severe acute pancreatitis," *Hepatobiliary & pancreatic diseases international*, vol. 9, no. 2, pp. 201–207, 2010.

[17] S. L. Deshmane, S. Kremlev, S. Amini, and B. E. Sawaya, "Monocyte chemoattractant protein-1 (MCP-1): an overview," *Journal of interferon & cytokine research*, vol. 29, no. 6, pp. 313–326, 2009.

[18] J. Yu, L. Ni, X. Zhang, J. Zhang, O. Abdel-Razek, and G. Wang, "Surfactant protein D dampens lung injury by suppressing NLRP3 inflammasome activation and NF-κB signaling in acute pancreatitis," *Shock*, vol. 51, no. 5, pp. 557–568, 2019.

[19] R. Wang, C. Y. Zhang, L. P. Bai et al., "Flavonoids derived from liquorice suppress murine macrophage activation by up- regulating heme oxygenase-1 independent of Nrf2 activation," *International Immunopharmacology*, vol. 28, no. 2, pp. 917–924, 2015.

[20] H. Honda, Y. Nagai, T. Matsunaga et al., "Isoliquiritigenin is a potent inhibitor of NLRP3 inflammasome activation and diet-induced adipose tissue inflammation," *Journal of leukocyte biology*, vol. 96, no. 6, pp. 1087–1100, 2014.

[21] Z. G. Luan, J. Zhang, X. H. Yin, X. C. Ma, and R. X. Guo, "Ethyl pyruvate significantly inhibits tumour necrosis factor-α, inter-leukin-1β and high mobility group box 1 releasing and attenuates sodium taurocholate-induced severe acute pancreatitis associated with acute lung injury," *Clinical and experimental immunology*, vol. 172, no. 3, pp. 417–426, 2013.

[22] S. M. Cha, J. D. Cha, E. J. Jang, G. U. Kim, and K. Y. Lee, "Sophoraflavanone G prevents _Streptococcus mutans_ surface antigen I/II- induced production of NO and PGE$_2$ by inhibiting MAPK- mediated pathways in RAW 264.7 macrophages," *Archives of oral biology*, vol. 68, pp. 97–104, 2016.

[23] Y. C. Hung, C. C. Hsu, C. H. Chung, and T. F. Huang, "The disintegrin, trimucrin, suppresses LPS-induced activation of phagocytes primarily through blockade of NF-κB and MAPK activation," *Naunyn-Schmiedeberg's archives of pharmacology*, vol. 389, no. 7, pp. 723–737, 2016.

[24] G. Kong, X. Huang, L. Wang et al., "Astilbin alleviates LPS-induced ARDS by suppressing MAPK signaling pathway and protecting pulmonary endothelial glycocalyx," *International Immunopharmacology*, vol. 36, pp. 51–58, 2016.

[25] T. T. Cornell, A. Fleszar, W. McHugh, N. B. Blatt, A. M. Le Vine, and T. P. Shanley, "Mitogen-activated protein kinase phosphatase 2, MKP-2, regulates early inflammation in acute lung injury," *American journal of physiology Lung cellular and molecular physiology*, vol. 303, no. 3, pp. L251–L258, 2012.

[26] J. T. Hsu, W. H. Kan, C. H. Hsieh, M. A. Choudhry, K. I. Bland, and I. H. Chaudry, "Role of extracellular signal-regulated protein kinase (ERK) in 17β-estradiol- mediated attenuation of lung injury after trauma-hemorrhage," *Surgery*, vol. 145, no. 2, pp. 226–234, 2009.

[27] Y. Chen, L. Wang, Q. Kang et al., "Heat shock protein A12B protects vascular endothelial cells against sepsis-induced acute lung injury in mice," *Cellular physiology and biochemistry*, vol. 42, no. 1, pp. 156–168, 2017.

[28] C. Chen, Y. Wang, Z. Zhang, C. Wang, and M. Peng, "Toll-like receptor 4 regulates heme oxygenase-1 expression after hemorrhagic shock induced acute lung injury in mice: requirement of p38 mitogen-activated protein kinase activation," *Shock*, vol. 31, no. 5, pp. 486–492, 2009.

[29] A. R. Kochanek, E. Y. Fukudome, Y. Li et al., "Histone Deacetylase Inhibitor Treatment Attenuates MAP Kinase Pathway Activation and Pulmonary Inflammation Following Hemorrhagic Shock in a Rodent Model[1]," *The Journal of surgical research*, vol. 176, no. 1, pp. 185–194, 2012.

[30] K. Y. Lv, X. Y. Yu, Y. S. Bai et al., "Role of inhibition of p38 mitogen-activated protein kinase in liver dysfunction after hemorrhagic shock and resuscitation," *The Journal of surgical research*, vol. 178, no. 2, pp. 827–832, 2012.

[31] S. Yu, J. Xie, Y. Xiang et al., "Downregulation of TNF-alpha/TNF-R1 signals by AT-Lipoxin A4 may be a significant mechanism of attenuation in SAP-associated lung injury," *Mediators of Inflammation*, vol. 2019, Article ID 9019404, 7 pages, 2019.

[32] H. B. Li, G. Z. Wang, J. Gong et al., "BML-111 attenuates hemorrhagic shock-induced acute lung injury through inhibiting activation of mitogen-activated protein kinase pathway in rats," *The Journal of surgical research*, vol. 183, no. 2, pp. 710–719, 2013.

[33] X. M. Wu, K. Q. Ji, H. Y. Wang et al., "Retracted: microRNA-542-5p protects against acute lung injury in mice with severe acute pancreatitis by suppressing the mitogen-activated protein kinase signaling pathway through the negative regulation of

of P21-activated kinase 1," *Journal of Cellular Biochemistry*, vol. 120, no. 1, pp. 290–304, 2019.

[34] W. Lv, C. Lv, S. Yu et al., "Lipoxin A4 attenuation of endothelial inflammation response mimicking pancreatitis-induced lung injury," *Experimental biology and medicine*, vol. 238, no. 12, pp. 1388–1395, 2013.

[35] V. Silei, V. Politi, and G. M. Lauro, "Uridine induces differentiation in human neuroblastoma cells via protein kinase C epsilon," *Journal of Neuroscience Research*, vol. 61, no. 2, pp. 206–211, 2000.

[36] I. Gutcher, P. R. Webb, and N. G. Anderson, "The isoform-specific regulation of apoptosis by protein kinase C," *Cellular and molecular life sciences*, vol. 60, no. 6, pp. 1061–1070, 2003.

[37] B. Bastani, L. Yang, J. J. Baldassare, D. A. Pollo, and J. D. Gardner, "Cellular distribution of isoforms of protein kinase C (PKC) in pancreatic acini," *Biochimica et Biophysica Acta*, vol. 1269, no. 3, pp. 307–315, 1995.

[38] J. Reibman, A. T. Talbot, Y. Hsu et al., "Regulation of expression of granulocyte-macrophage colony-stimulating factor in human bronchial epithelial cells: roles of protein kinase C and mitogen-activated protein kinases," *Journal of immunology*, vol. 165, no. 3, pp. 1618–1625, 2000.

[39] S. Akakura, P. Nochajski, L. Gao, P. Sotomayor, S. Matsui, and I. H. Gelman, "Rb-dependent cellular senescence, multinucleation and susceptibility to oncogenic transformation through PKC scaffolding by SSeCKS/AKAP12," *Cell Cycle*, vol. 9, no. 23, pp. 4656–4665, 2010.

[40] B. Shao, C. Li, H. Yang et al., "The relationship between Src-suppressed C kinase substrate and β-1,4 galactosyltransferase-I in the process of lipopolysaccharide-induced TNF-α secretion in rat primary astrocytes," *Cellular and molecular neurobiology*, vol. 31, no. 7, pp. 1047–1056, 2011.

[41] P. F. Cezar-de-Mello, A. M. Vieira, V. Nascimento-Silva, C. G. Villela, C. Barja-Fidalgo, and I. M. Fierro, "ATL-1, an analogue of aspirin-triggered lipoxin A4, is a potent inhibitor of several steps in angiogenesis induced by vascular endothelial growth factor," *British journal of pharmacology*, vol. 153, no. 5, pp. 956–965, 2008.

[42] B. Li, X. Han, X. Ye et al., "Substance P-regulated leukotriene B4 production promotes acute pancreatitis- associated lung injury through neutrophil reverse migration," *International Immunopharmacology*, vol. 57, pp. 147–156, 2018.

[43] Z. Shi, W. Ye, J. Zhang et al., "LipoxinA4 attenuates acute pancreatitis-associated acute lung injury by regulating AQP-5 and MMP-9 expression, anti-apoptosis and PKC/SSeCKS-mediated F-actin activation," *Molecular immunology*, vol. 103, pp. 78–88, 2018.

[44] S. Katz, M. Hukkanen, K. Lounatmaa, P. Rousselle, T. Tervo, and I. Virtanen, "Cooperation of isoforms of laminin-332 and tenascin-C^L during early adhesion and spreading of immortalized human corneal epithelial cells," *Experimental eye research*, vol. 83, no. 6, pp. 1412–1422, 2006.

[45] P. Mydel, J. M. Shipley, T. L. Adair-Kirk et al., "Neutrophil Elastase Cleaves Laminin-332 (Laminin-5) Generating Peptides That Are Chemotactic for Neutrophils," *The Journal of biological chemistry*, vol. 283, no. 15, pp. 9513–9522, 2008.

[46] C. Xu, J. Zhang, J. Liu et al., "Proteomic analysis reveals the protective effects of emodin on severe acute pancreatitis induced lung injury by inhibiting neutrophil proteases activity," *Journal of Proteomics*, vol. 220, p. 103760, 2020.

[47] R. Hoque, A. F. Malik, F. Gorelick, and W. Z. Mehal, "Sterile inflammatory response in acute pancreatitis," *Pancreas*, vol. 41, no. 3, pp. 353–357, 2012.

[48] J. M. Sanz, P. Chiozzi, D. Ferrari et al., "Activation of microglia by amyloid {beta} requires P2X7 receptor expression," *Journal of immunology*, vol. 182, no. 7, pp. 4378–4385, 2009.

[49] H. Xu, C. Xiong, L. He et al., "Trans-resveratrol attenuates high fatty acid-induced P2X7 receptor expression and IL-6 release in PC12 cells: possible role of P 38 MAPK pathway," *Inflammation*, vol. 38, no. 1, pp. 327–337, 2015.

[50] Q. Chen, H. Wu, S. Qin et al., "The P2X7 receptor involved in gp120-induced cell injury in BV2 microglia," *Inflammation*, vol. 39, no. 5, pp. 1814–1826, 2016.

[51] A. L. Giuliani, A. C. Sarti, S. Falzoni, and F. Di Virgilio, "The P2X7 receptor-interleukin-1 liaison," *Frontiers in pharmacology*, vol. 8, p. 123, 2017.

[52] F. Albalawi, W. Lu, J. M. Beckel, J. C. Lim, S. A. McCaughey, and C. H. Mitchell, "The P2X7 receptor primes IL-1β and the NLRP3 inflammasome in astrocytes exposed to mechanical strain," *Frontiers in cellular neuroscience*, vol. 11, p. 227, 2017.

[53] N. Yue, H. Huang, X. Zhu et al., "Activation of P2X7 receptor and NLRP3 inflammasome assembly in hippocampal glial cells mediates chronic stress-induced depressive-like behaviors," *Journal of Neuroinflammation*, vol. 14, no. 1, p. 102, 2017.

[54] Y. S. Kim, Y. M. Lee, T. I. Oh et al., "Emodin sensitizes hepatocellular carcinoma cells to the anti-cancer effect of sorafenib through suppression of cholesterol metabolism," *International journal of molecular sciences*, vol. 19, no. 10, p. 3127, 2018.

[55] J. W. Han, D. W. Shim, W. Y. Shin et al., "Anti-inflammatory effect of emodin via attenuation of NLRP3 inflammasome activation," *International journal of molecular sciences*, vol. 16, no. 12, pp. 8102–8109, 2015.

[56] D. Kim, G. Pertea, C. Trapnell, H. Pimentel, R. Kelley, and S. L. Salzberg, "TopHat2: accurate alignment of transcriptomes in the presence of insertions, deletions and gene fusions," *Genome biology*, vol. 14, no. 4, p. R36, 2013.

[57] M. N. Cabili, C. Trapnell, L. Goff et al., "Integrative annotation of human large intergenic noncoding RNAs reveals global properties and specific subclasses," *Genes & development*, vol. 25, no. 18, pp. 1915–1927, 2011.

[58] C. Trapnell, A. Roberts, L. Goff et al., "Differential gene and transcript expression analysis of RNA-seq experiments with TopHat and Cufflinks," *Nature protocols*, vol. 7, no. 3, pp. 562–578, 2012.

[59] L. Kong, Y. Zhang, Z. Q. Ye et al., "CPC: assess the protein-coding potential of transcripts using sequence features and support vector machine," *Nucleic acids research*, vol. 35, suppl_2, pp. W345–W349, 2007.

[60] J. Yao, S. Peng, J. Xu, and J. Fang, "Reversing ROS-mediated neurotoxicity by chlorogenic acid involves its direct antioxidant activity and activation of Nrf2-ARE signaling pathway," *BioFactors*, vol. 45, no. 4, pp. 616–626, 2019.

[61] M. Jin, J. Wang, X. Ji et al., "MCUR1 facilitates epithelial-mesenchymal transition and metastasis via the mitochondrial calcium dependent ROS/Nrf2/Notch pathway in hepatocellular carcinoma," *Journal of experimental & clinical cancer research*, vol. 38, no. 1, p. 136, 2019.

[62] Y. Dai, J. Zhang, J. Xiang, Y. Li, D. Wu, and J. Xu, "Calcitriol inhibits ROS-NLRP3-IL-1β signaling axis via activation of Nrf2-antioxidant signaling in hyperosmotic stress stimulated

human corneal epithelial cells," *Redox biology*, vol. 21, p. 101093, 2019.

[63] H. Lv, Q. Liu, Z. Wen, H. Feng, X. Deng, and X. Ci, "Xanthohumol ameliorates lipopolysaccharide (LPS)-induced acute lung injury via induction of AMPK/GSK3β-Nrf2 signal axis," *Redox biology*, vol. 12, pp. 311–324, 2017.

[64] W. Yao, G. Luo, G. Zhu et al., "Propofol activation of the Nrf2 pathway is associated with amelioration of acute lung injury in a rat liver transplantation model," *Oxidative medicine and cellular longevity*, vol. 2014, Article ID 258567, 9 pages, 2014.

[65] G. Zheng, H. Ren, H. Li et al., "_Lycium barbarum_ polysaccharide reduces hyperoxic acute lung injury in mice through Nrf2 pathway," *Biomedicine & pharmacotherapy = Biomedecine & pharmacotherapie*, vol. 111, pp. 733–739, 2019.

[66] V. O. Tkachev, E. B. Menshchikova, and N. K. Zenkov, "Mechanism of the Nrf2/Keap1/ARE signaling system," *Biochemistry. Biokhimiia*, vol. 76, no. 4, pp. 407–422, 2011.

[67] A. Peairs, A. Radjavi, S. Davis et al., "Activation of AMPK inhibits inflammation in MRL/lpr mouse mesangial cells," *Clinical and experimental immunology*, vol. 156, no. 3, pp. 542–551, 2009.

[68] L. Wang, S. Zhang, H. Cheng, H. Lv, G. Cheng, and X. Ci, "Nrf2-mediated liver protection by esculentoside A against acetaminophen toxicity through the AMPK/Akt/GSK3β pathway," *Free radical biology & medicine*, vol. 101, pp. 401–412, 2016.

[69] X. Liu, Q. Zhu, M. Zhang et al., "Isoliquiritigenin ameliorates acute pancreatitis in mice via inhibition of oxidative stress and modulation of the Nrf2/HO-1 pathway," *Oxidative medicine and cellular longevity*, vol. 2018, Article ID 7161592, 12 pages, 2018.

[70] B. S. Nasir, C. Landry, A. Menaouar et al., "HSP90 inhibitor improves lung protection in porcine model of donation after circulatory arrest," *The Annals of thoracic surgery*, vol. 110, no. 6, pp. 1861–1868, 2020.

[71] D. R. Calabrese, E. Aminian, B. Mallavia et al., "Natural killer cells activated through NKG2D mediate lung ischemia-reperfusion injury," *The Journal of clinical investigation*, vol. 131, no. 3, 2021.

[72] E. Akpinar, Z. Kutlu, D. Kose et al., "Protective effects of idebenone against sepsis induced acute lung damage," *Journal of investigative surgery*, vol. 2021, pp. 1–9, 2021.

[73] J. M. Leonard, C. X. Zhang, L. Lu et al., "Extrathoracic multiple trauma dysregulates neutrophil function and exacerbates pneumonia-induced lung injury," *The journal of trauma and acute care surgery*, vol. 90, no. 6, pp. 924–934, 2021.

[74] J. W. Semple, J. Rebetz, and R. Kapur, "Transfusion-associated circulatory overload and transfusion-related acute lung injury," *Blood*, vol. 133, no. 17, pp. 1840–1853, 2019.

[75] J. W. Semple and R. Kapur, "The contribution of recipient platelets in TRALI: has the jury reached a verdict?," *Transfusion*, vol. 60, no. 5, pp. 886–888, 2020.

Research Article

A Nomogram Prediction of Length of Hospital Stay in Patients with COVID-19 Pneumonia: A Retrospective Cohort Study

Kang Li ⬥, Chi Zhang, Ling Qin, Chaoran Zang, Ang Li, Jianping Sun, Yan Zhao, Yingmei Feng, and Yonghong Zhang ⬥

Beijing You'An Hospital, Capital Medical University, Beijing, China

Correspondence should be addressed to Yonghong Zhang; zhangyh@ccmu.edu.cn

Assessing the length of hospital stay (LOS) in patients with coronavirus disease 2019 (COVID-19) pneumonia is helpful in optimizing the use efficiency of hospital beds and medical resources and relieving medical resource shortages. This retrospective cohort study of 97 patients was conducted at Beijing You'An Hospital between January 21, 2020, and March 21, 2020. A multivariate Cox proportional hazards regression based on the smallest Akaike information criterion value was used to select demographic and clinical variables to construct a nomogram. Discrimination, area under the receiver operating characteristic curve (AUC), calibration, and Kaplan–Meier curves with the log-rank test were used to assess the nomogram model. The median LOS was 13 days (interquartile range [IQR]: 10–18). Age, alanine aminotransferase, pneumonia, platelet count, and PF ratio (PaO_2/FiO_2) were included in the final model. The C-index of the nomogram was 0.76 (95%confidence interval [CI] = 0.69 – 0.83), and the AUC was 0.88 (95%CI = 0.82 – 0.95). The adjusted C-index was 0.75 (95%CI = 0.67 – 0.82) and adjusted AUC 0.86 (95%CI = 0.73 – 0.95), both after 1000 bootstrap cross internal validations. A Brier score of 0.11 (95%CI = 0.07 – 0.15) and adjusted Brier score of 0.130 (95%CI = 0.07 – 0.20) for the calibration curve showed good agreement. The AUC values for the nomogram at LOS of 10, 20, and 30 days were 0.79 (95%CI = 0.69 – 0.89), 0.89 (95%CI = 0.83 – 0.96), and 0.96 (95%CI = 0.92 – 1.00), respectively, and the high fit score of the nomogram model indicated a high probability of hospital stay. These results confirmed that the nomogram model accurately predicted the LOS of patients with COVID-19. We developed and validated a nomogram that incorporated five independent predictors of LOS. If validated in a future large cohort study, the model may help to optimize discharge strategies and, thus, shorten LOS in patients with COVID-19.

1. Introduction

Coronaviruses (CoVs) are a large family of single-stranded RNA viruses, and beta-CoVs have caused international outbreaks of emerging respiratory diseases, including severe acute respiratory syndrome coronavirus (SARS-CoV) in 2003 [1, 2] and Middle East respiratory syndrome-CoV (MERS-CoV) in 2012 [3]. In December 2019, a novel severe acute respiratory syndrome coronavirus 2 (SARS-CoV-2) infection in Wuhan led to coronavirus disease 2019 (COVID-19), with more than 290,000 confirmed cases in 174 countries and approximately 12,000 deaths (as of March

21, 2020) [4, 5]. The infectious disease outbreak led to a substantial increase in the demand for hospital beds, a shortage of medical equipment, and possible nosocomial infection among medical staff. According to the clinical condition of patients, physicians can evaluate the length of hospital stay (LOS), which is helpful in relieving medical resource shortages. A recent study reported a model including five variables, namely, procalcitonin, heart rate, Wuhan traveling history, lymphocyte count, and cough to predict prolonged LOS (>14 days) [6]. However, the model could only predict whether the LOS was >14 days. However, the "Wuhan traveling history" variable limited the extrapolative application

of this model because the COVID-19 epidemic had been eliminated in Wuhan city.

We conducted a retrospective cohort study on the clinical characteristics of cured and discharged patients with confirmed COVID-19 infection between January 21, 2020, and March 21, 2020, in Beijing. We applied Cox proportional hazards regression to analyze time- (LOS-) to-event (discharge) data, which was able to provide individualized predictions of the estimated time to the event of interest. This study is aimed at describing the clinical characteristics of and develop and internally validate a predictive nomogram for estimating the LOS in patients with COVID-19.

2. Materials and Methods

2.1. Cohort Construction. This was a single-center, retrospective cohort study enrolling consecutive COVID-19 pneumonia patients aged over 18 years who underwent treatment at Beijing You'An Hospital between January 21, 2020, and March 21, 2020. All patients with COVID-19 pneumonia were diagnosed and classified according to the new coronavirus pneumonia diagnosis and treatment plan (trial version 6, in Chinese) developed by the National Health Committee of the People's Republic of China (http://www.nhc.gov.cn/). This study was approved by the Ethics Committee of Beijing You'An Hospital, and informed consent was obtained from all the patients.

2.2. Outcomes and Selection of Covariates. The primary outcome was LOS, which was defined as the time in days from hospital admission to discharge and was considered as "event =1" in Cox analysis. Readmission within two weeks was considered a prolonged LOS, and it was counted from the first hospitalization day. Death before discharge was also considered as a prolonged LOS and was estimated to be 800 days (longer than the longest LOS) and censored with "event = 0" in Cox analysis. Patients who died within 24 h of admission to the hospital were excluded from the Cox analysis. All patients were followed up for at least 6 months after discharge.

We collected baseline data, including demographic characteristics (age, sex, and comorbid diseases), epidemiological history, laboratory tests (biochemical indicators, routine blood testing, C-reactive protein, and chest radiograph or computed tomography [CT] scan), treatment, and outcome data. The data were extracted from the electronic medical record system, laboratory information system, and picture archiving and communication system.

2.3. Statistical Analysis. Continuous and categorical variables are presented as medians with interquartile ranges (IQRs) and n (%), respectively. We used Fisher's exact test or the chi-square test and the Mann–Whitney U test to make between-group comparisons of the subjects in the three groups. A backward stepwise method based on the smallest Akaike information criterion (AIC) value was applied to select covariates to be included in the Cox proportional hazards models.

The nomogram was developed using the "rms" R package. The area under the time-dependent receiver operating characteristic (ROC) curve was obtained using the "survival ROC" package. Harrell's C-index (concordance statistic, or C-statistic) was used to assess the predictive capacity of the nomogram. Bias-corrected calibration using the bootstrapping method with 1000 resamples was used for internal validation of the nomogram. Based on the scores of each variable, the total scores for each patient could be calculated using the "pec" package in R. The fit score of the five-covariate combination was used to stratify patients for Kaplan–Meier curve analysis using the log-rank test to compare the probability of hospital stay among the different groups, and the "survminer" package was applied in this regard. Statistical analyses were performed using R version 3.6.2. Extension packages, including "ggplot2," "foreign," and "export," were also employed.

3. Results

3.1. Patient Population. A total of 102 patients were diagnosed with COVID-19 between January 21, 2020, and March 21, 2020, and treated at Beijing You'An Hospital. One patient who died within 24 h and four who were under 18 years of age were excluded from the analysis. Therefore, a total of 97 patients, including 84 (86.6%) discharged and 13 undischarged patients (including four deceased and four readmitted patients), were included in this study (Figure 1(a)). After at least 6 months of follow-up after discharge, there was no death. The baseline demographic characteristics of the study cohort are presented in Table 1. The median age of the study patients was 51.51 years (IQR: 38–64), and 42.3% were men. The primary outcome was LOS, and the median LOS was 13 days (IQR: 10–18). The LOS distribution of the discharged COVID-19 pneumonia patients is shown in Figure 1(b).

The LOS increased with age, and there was a significant difference among the three groups. The percentage of neutrophils, percentage of lymphocytes, platelet-to-lymphocyte ratio (PLR), and neutrophil-to-lymphocyte ratio (NLR) was significantly different among the three groups (all $p < 0.01$). The number of subjects with normal ALT and AST levels (both < 40 U/L) in the third group (LOS ≥ 19 days) was significantly lower than those in the other groups ($p = 0.009$ and $p \le 0.001$, respectively). Myoglobin and lactate levels in the third group (LOS ≥ 19 days) were significantly higher than those in the other groups ($p \le 0.001$ and $p = 0.004$, respectively).

3.2. Independent Predictors of LOS in Univariate and Multivariate Analysis. We assessed the LOS using Cox proportional hazard regression. Older age (≥50 years), high levels of ALT and AST (both ≥ 40 U/L), critical and severe pneumonia, and high levels of myoglobin (≥100 μg/L) significantly increased the chance of longer LOS (all $p < 0.05$). In contrast, female sex, high platelet count (≥300 × 10^9/L), high lymphocyte count (≥0.8 × 10^9/L), high PF ratio (≥300 mmHg), and gradual increase in the glomerular filtration rate were significantly associated with shorter LOS (all $p < 0.05$). The
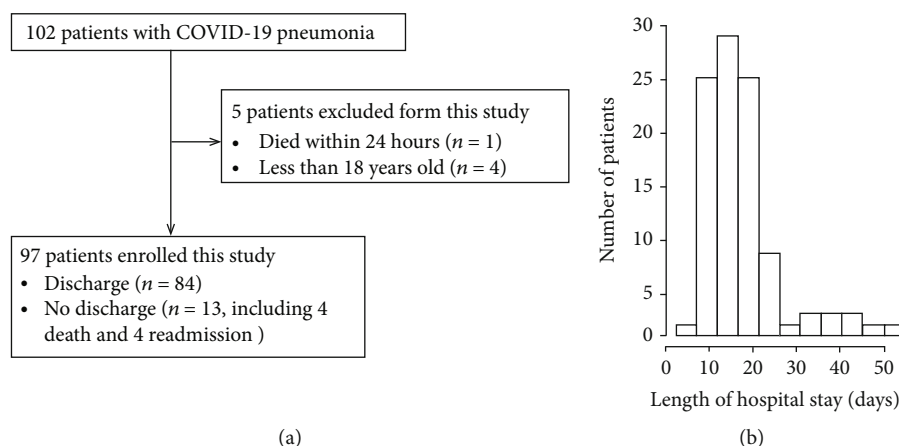
FIGURE 1: (a) Flow diagram of patient enrollment. (b) Distribution of length of hospital stay of discharged COVID-19 pneumonia patients.

other independent risk factors in the univariate analysis are shown in Table 2.

After backward elimination and model selection based on AIC, age (hazard ratio [HR] = 0.49; 95%confidence interval [CI] = 0.29 – 0.83, $p = 0.00734$), pneumonia (HR = 0.31, 95% CI = 0.18 – 0.52, $p = 1.73e - 05$), ALT (HR = 0.49, 95%CI = 0.29 – 0.83, $p = 0.00697$), PF ratio (HR = 1.45, 95%CI = 1.21 – 1.97, $p = 0.0413$), and platelet count (HR = 1.77, 95%CI = 0.93 – 3.39, $p = 0.082$) were included in the final model (smallest AIC value = 600.81) for the development of the nomogram (Table 2).

3.3. Development and Internal Validation of LOS-Predicting Nomogram. Five independently associated risk factors were used to form an LOS risk-estimating nomogram (Figure 2(a)). The nomogram demonstrated favorable accuracy in estimating the probability of hospital stay, with C-index values of 0.76 (95%CI = 0.69 – 0.83) and AUC of 0.88 (95%CI = 0.82 – 0.95) (Figure 2(b)). The overfit of the model was estimated by applying the bootstrap internal validation method. The adjusted C-index was 0.75 (95%CI = 0.67 – 0.82) and adjusted AUC 0.86 (95%CI = 0.73 – 0.95) after 1000 bootstrap crossvalidation iterations (Figure 2(c)), which represented the bias-corrected estimate of model performance in the future and demonstrated favorable predictive accuracy for the nomogram. A Brier score of 0.11 (95%CI = 0.07 – 0.15) and adjusted Brier score of 0.13 (95%CI = 0.07 – 0.20) for the calibration curve demonstrated favorable agreement between prediction probability by nomogram and actual state of hospitalization (Figure 2(c)).

Finally, the area under the time-dependent ROC curve was used to validate the ability of the nomogram to discriminate patients who were discharged within 10, 20, and 30 days of hospital stay. The AUC values for the nomogram at 10, 20, and 30 days were 0.79 (95%CI = 0.69 – 0.89), 0.89 (95%CI = 0.83 – 0.96), and 0.96 (95%CI = 0.92 – 1.00), respectively (Figure 3(a)). The Brier score of the calibration curve for the nomogram at 10, 20, and 30 days was 0.16 (95%CI = 0.10 – 0.21), 0.10 (95%CI = 0.07 – 0.14), and 0.06 (95%CI = 0.03 – 0.08), respectively (Figure 3(b)). The Kaplan–Meier

curves together with the log-rank test also demonstrated that a high fit score nomogram model indicated a high probability of long hospital stay in the training group (Figure 3(c), log-rank $p < 0.0001$). These results confirmed that the nomogram model accurately predicted the LOS of patients with COVID-19.

4. Discussion

COVID-19 has emerged as a worldwide pandemic; at present, the number of infected people continually increases substantially every day in most countries of the world. According to patient clinical data, physicians can evaluate their length of stay. It is beneficial to optimize the use efficiency of hospital beds and medical resources and relieve medical resource shortages.

In this retrospective cohort study, we found that the median LOS was 13 days (IQR: 10–18). Age, ALT, PF ratio, pneumonia, and platelet count were independently associated with LOS in patients with COVID-19, and they were included in the final nomogram. The prognostic model demonstrated a significantly higher predictive accuracy and discriminative ability for the prediction of 10-, 20-, and 30-day LOS for COVID-19-infected patients. Further, the nomogram demonstrated favorable discrimination and superior performance in internal validation. The nomogram model with a high fit score indicated a high probability of hospital stay. These results confirmed that the nomogram model accurately predicted the LOS of patients with COVID-19.

Older age is an important independent predictor of mortality [7]. Similar results were obtained for SARS [1, 8] and MERS [9]. Both cell-mediated immunity and humoral immune function evidently declined in elderly patients. Concomitantly, cytokine and chemokine signaling networks in elderly patients changed; type 2 cytokine response tended to be more sensitive than type 1 [10], and the proportion of T cells producing IL-4, IL-8, and IL-10 increased with age [11]. In these cases, viral replication and longer-lasting proinflammatory responses were not controlled. In SARS-CoV and MERS-CoV infection, uncontrolled induction of proinflammatory cytokines resulted in pathogenesis and disease

TABLE 1: Summary statistics of patient demographics and clinical characteristics (by quartile of LOS).

	Total	≤10 days (n = 26)	11–18 days (n = 49)	≥19 days (n = 22)	p value
Demographic characteristics					
Age, years (IQR)	51.5 (38–64)	41.0 (31,62.5)	49 (37–60)	63 (57–74.8)	≤0.001***
Male sex, n (%)	41 (42.3)	9 (34.6)	18 (36.7)	14 (63.6)	0.069
Clinical findings					
Pneumonia, n (%)					
Mild	69 (71.1)	23 (88.5)	39 (79.6)	7 (31.8)	≤0.001***
Severe	17 (17.5)	3 (11.5)	8 (16.3)	6 (27.3)	
Critical	11 (11.3)	0 (0.0)	2 (4.1)	9 (40.9)	
Fever (°C), n (%)					
<37.3	24 (24.7)	11 (42.3)	11 (22.4)	2 (9.1)	0.045*
37.3–38.5	50 (51.5)	13 (50.0)	24 (49.0)	13 (59.1)	
>38.5	23 (23.7)	2 (7.7)	14 (28.6)	7 (31.8)	
Cough	58 (59.8%)	13 (46.4%)	31 (62%)	15 (68.2%)	0.423
Sputum	25 (25.8%)	5 (19.2%)	12 (24.5%)	8 (36.4%)	0.384
Vomiting	4 (4.1%)	1 (3.8%)	2 (4.1%)	1 (4.5%)	0.993
Diarrhea	2 (2.1%)	1 (3.8%)	0 (0%)	1 (4.5%)	0.238
Lung CT[a]	85 (87.6%)	21 (80.8%)	44 (91.8%)	19 (86.4%)	0.384
Coexisting illnesses					
Kidney disease	3 (3.1%)	1 (3.80%)	2 (4.1%)	0 (0.0%)	0.455
Hypertension	22 (22.7%)	2 (15.4%)	9 (18.4%)	9 (40.9%)	0.081
Hyperlipidemia	3 (3.1%)	1 (3.8%)	1 (2.0%)	1 (4.5%)	0.825
Diabetes	8 (8.2%)	2 (7.7%)	4 (8.2%)	3 (13.6%)	0.984
Heart disease	10 (10.3%)	2 (7.7%)	5 (10.2%)	2 (10.5%)	0.798
Lung disease	7 (7.2%)	2 (7.7%)	4 (8.2%)	1 (4.5%)	0.844
Surgery	22 (22.7%)	4 (15.4%)	12 (24.5%)	6 (27.3%)	0.564
Laboratory indicators					
White blood cell count, ×10⁹/L	4.4 (3.5–5.9)	4.1 (3.5–5.8)	4.4 (3.5–5.7)	5.0 (3.2–6.9)	0.583
<4	40 (41.2%)	12 (46.2%)	20 (40.8%)	8 (36.4%)	0.787
≥4	57 (58.8%)	14 (53.8%)	29 (59.2%)	14 (63.6%)	
Hemoglobin, g/dL	136 (125–144)	131 (120.3–144.3)	135 (126–143.5)	139 (129–149)	0.157
Platelet count × 10⁹/L	194 (160–238)	206 (161–298.3)	193 (144.5–245)	191 (147.5–226.3)	0.257
<100	5 (5.2%)	0 (0.0%)	2 (4.1%)	5 (10.2%)	0.071
100–300	80 (82.5%)	20 (76.9%)	42 (85.7%)	6 (23.1%)	
>300	12 (12.4%)	6 (23.1%)	5 (10.2%)	1 (4.5%)	
Lymphocyte count × 10⁹/L	1.1 (0.77–1.53)	1.26 (0.93–1.61)	1.18 (0.80–1.54)	0.81 (0.70–1.21)	0.026*
<0.8	26 (26.8%)	5 (19.2%)	11 (22.4%)	10 (45.5%)	0.90
≥0.8	71 (73.2%)	21 (80.8%)	38 (77.6%)	12 (54.5%)	
Monocyte count×10⁹/L	0.31 (0.21–0.44)	0.34 (0.22–0.42)	0.25 (0.16–0.39)	0.32 (0.19–0.51)	0.928
Neutrophil count × 10⁹/L	2.69 (1.84–4.09)	2.37 (1.86–3.42)	2.69 (1.84–3.83)	3.71 (1.68–5.38)	0.067
<1.8	21 (21.6%)	5 (19.2%)	10 (20.4%)	6 (27.3%)	0.206
1.8–6.3	70 (72.2%)	21 (80.8%)	36 (73.5%)	13 (59.1%)	
>6.3	6 (6.2%)	0 (0%)	3 (6.1%)	3 (13.6%)	
Lymphocyte percentage	26.1 (17.9–34.5)	33 (21.7–37.8)	26.1 (19.3–34.3)	18.7 (19.3–34.5)	0.002**
<20	29 (29.9%)	3 (11.5%)	14 (28.6%)	12 (54.5%)	0.007**
20–40	58 (59.8%)	19 (73.1%)	29 (59.2%)	10 (45.5%)	
>40	10 (10.3%)	4 (15.4%)	6 (12.2%)	0 (0.0%)	

TABLE 1: Continued.

	Total	≤10 days ($n = 26$)	11–18 days ($n = 49$)	≥19 days ($n = 22$)	p value
Neutrophil percentage	64.0 (51.8–72.3)	55.4 (49.2–69.1)	64 (53.1–72.7)	70.4 (60.4–79.6)	0.002**
<75	78 (80.4%)	25 (96.2%)	39 (79.6%)	14 (63.6%)	0.018*
≥75	19 (19.6%)	1 (3.8%)	10 (20.4%)	8 (36.4%)	
NLR	2.4 (1.4, 3.9)	1.7 (1.3–3.1)	2.3 (1.6–3.8)	3.61 (1.8–6.3)	0.004**
<2.75	56 (57.7%)	18 (69.2%)	31 (63.3%)	7 (31.8%)	0.018*
2.75	41 (42.3%)	8 (30.8%)	18 (36.7%)	15 (68.2%)	
LMR	3.7 (2.8, 5.3)	4.1 (2.9, 6.3)	3.9 (2.8, 5.4)	3.0 (2.3,4.8)	0.268
<2.63	20 (20.8%)	5 (19.2%)	7 (14.3%)	8 (38.1%)	0.096
≥2.63	76 (79.2%)	21 (80.8%)	42 (85.7%)	8 (61.9%)	
PLR	177.3 (124.8–246.2)	132.7 (118.5–172.3)	188.1 (124.8–156.6)	221.5 (163.6–182.5)	0.018*
<160	41 (42.3%)	15 (57.7%)	21 (42.9%)	5 (22.7%)	0.045
≥160	56 (57.7%)	11 (42.3%)	28 (57.1%)	17 (77.3%)	
Prothrombin time, s	12.6 (12.1–131.1)	12.8 (12.2–13.4)	12.4 (11.9–12.87)	12.75 (12.1–13.42)	0.417
Prothrombin activity, percentage	75 (71–80)	73.5 (68.5–79.0)	76.0 (73.0–82.0)	74.0 (68.5–78.5)	0.459
<75	46 (48.4%)	15 (57.7%)	19 (39.6%)	12 (57.1%)	0.219
≥75	49 (51.6%)	11 (43.3%)	29 (60.4%)	9 (42.9%)	
C-reactive protein, mg/L	14.7 (3.4–37.4)	12.7 (2.0–18.3)	16.8 (3.3, 41.15)	19.4 (10.0–54.13)	0.314
Procalcitonin, ug/L	0.11 (0.10–0.14)	0.10 (0.08–0.15)	0.11 (0.06, 0.15)	0.12 (0.10–0.14)	0.256
Fibrinogen, g/L	3.2 (2.5–4.3)	3.0 (2.5–4.3)	3.2 (2.5–4.1)	3.2 (2.5–4.4)	0.549
ALT, U/L	28 (20–45)	26.5 (20–39)	26 (20–42)	42 (19.7–52.7)	0.126
<40	65 (67.0%)	21 (80.8%)	35 (71.4%)	9 (40.9%)	0.009**
≥40	32 (33.0%)	5 (19.2%)	14 (28.6%)	13 (59.1%)	
AST, U/L	30 (21.5–42)	25.5 (20.5–34)	28.0 (21–40)	42.5 (22.75–64.5)	0.004**
<40	70 (72.2%)	24 (92.3%)	38 (77.6%)	3 (36.4%)	≤0.001***
≥40	27 (27.8%)	2 (7.7%)	11 (22.4%)	14 (63.6%)	
AST/ALT	1.04 (0.76–1.35)	0.96 (0.60, 1.43)	1.02 (0.73–1.30)	1.30 (0.89, 1.71)	0.108
Total bilirubin, mmol/L	9.60 (7.10–13.05)	8.80 (6.13–12.10)	9.20 (6.80–12.60)	12.35 (9.38–14.75)	0.046*
Albumin, g/L	36.8 (33–39.8)	37.60 (33.8–40)	36.6 (33.4–39.9)	36.2 (32.5–40)	0.158
<35	36 (37.1%)	8 (30.8%)	17 (34.7%)	11 (50.0%)	0.350
≥35	61 (62.9%)	18 (69.2%)	32 (65.3%)	11 (50.0%)	
Glomerular filtration rate, (mL/min)	99.5 (91–113.75)	109.35 (94.8–119.7)	105.3 (94.2–117.6)	94.5 (80.3–97.4)	0.001**
Carbon dioxide combining power, mmol/L	26.8 (24.4–28.9)	25.70 (24.4–28.3)	27.2 (24.7–28.9)	27 (23–28.9)	0.428
Creatine kinase, U/L	72 (46–118)	59 (42–100.3)	72 (46–118)	118 (59.3–353)	0.203
<185	83 (85.6%)	25 (96.2%)	43 (87.8%)	15 (68.2%)	0.022*
≥185	14 (14.4%)	1 (3.8%)	6 (12.2%)	7 (31.8%)	
Creatine kinase isoenzymes, CK-MB, ng/mL	0.34 (0.16–0.73)	0.29 (0.08–0.61)	0.28 (0.13–0.69)	0.57 (0.27–1.10)	0.008**
<5	66 (68.0%)	17 (65.4%)	39 (79.6%)	10 (45.5%)	0.016**
≥5	31 (32.0%)	9 (34.6%)	10 (20.4%)	12 (54.5%)	
Myoglobin, μg/L	45 (30–66)	34 (27.5–50)	38 (29–60.5)	66 (49.5–187.5)	≤0.001***
<100	84 (86.6%)	24 (92.3%)	46 (93.9%)	14 (63.6%)	0.004**
≥100	13 (13.4%)	2 (7.7%)	3 (6.1%)	8 (36.4%)	
Lactate, mmol/L	1.2 (0.9–1.7)	1.0 (0.9–1.2)	1.24 (0.9–1.7)	1.6 (1.2–1.9)	0.004**
<1.7	69 (73.4%)	22 (88.0%)	37 (78.7%)	10 (45.5%)	0.02*
≥1.7	25 (26.6%)	3 (12.0%)	10 (21.3%)	12 (54.5%)	

TABLE 1: Continued.

	Total	≤10 days (n = 26)	11–18 days (n = 49)	≥19 days (n = 22)	p value
PF ratio, mmHg	433.5 (311.4–527.4)	471.3 (293.5–530.8)	446 (370.8–572.9)	340 (223.4–447.4)	0.02*
<300	20	7	4	9	0.003**
≥300	77	19	45	13	
Treatment					
Antibiotics	30 (30.9%)	11 (42.3%)	13 (26.5%)	6 (27.3%)	0.340
Antiviral treatment	37 (38.1%)	10 (38.5%)	19 (38.8%)	8 (36.4%)	0.981
Chinese medicine treatment	74 (76.3%)	22 (84.6%)	36 (73.5%)	16 (72.7%)	0.505
Corticosteroids	19 (19.6%)	0 (0.0%)	8 (16.3%)	11 (50.0%)	≤0.001***
Oxygen therapy	34 (35.1%)	4 (15.4%)	19 (38.8%)	11 (50.0%)	0.032*
Ventilator	6 (6.2%)	0 (0.0%)	2 (4.1%)	4 (18.2%)	0.024*

[a]Positive result: CT images showing multiple patchy ground-glass opacities along the peribronchial and subpleural lungs; NLR: neutrophil-to-lymphocyte ratio; LMR: lymphocyte-to-monocyte ratio; PLR: platelet-to-lymphocyte ratio; ALT: alanine aminotransferase; AST: aspartate aminotransferase; PF ratio: PaO_2/FiO_2 ratio. Significance codes: "***"0.001, "**"0.01, "*"0.05.

TABLE 2: Prognostic factors associated with LOS in COVID-19 pneumonia.

Variables	Univariate		Multivariate	
	HR (95% CI)	p value	HR (95% CI)	p value
Age, years (≥50 vs. < 50)	0.58 (0.33–1.01)	3.22e-04***	0.49 (0.29–0.83)	0.00734**
Sex (female vs. male)	1.89 (1.71–3.25)	0.0077*		
ALT, U/L (≥40 vs. <40)	0.45 (0.33–0.87)	0.0065*	0.49 (0.29–0.83)	0.00697**
AST, U/L (≥40 vs. <40)	0.42 (0.23–0.78)	3.34e-03**		
Fever (°C) (≥37.3 vs. < 37.3)	0.58 (0.35–1.08)	0.39		
Pneumonia (critical + severe vs. mild)	0.33 (0.049–0.47)	1.52e-03**	0.31 (0.18–0.52)	1.73e-05***
Hemoglobin, g/L (per unit)	0.97 (0.96–0.99)	0.034*		
Lymphocyte count × 10⁹/L (≥0.8 vs. < 0.8)	1.55 (0.78–2.51)	0.026*		
Neutrophil count × 10⁹/L (per unit)	0.96 (0.84–1.16)	0.047*		
Platelet count ×10⁹/L (≥300 vs. <300)	2.52 (0.69–7.55)	0.012*	1.77 (0.93–3.39)	0.08201
NLR (≥2.75 vs. < 2.75)	0.77 (0.66–1.20)	0.22		
C-reactive protein, mg/L (≥2.2 vs. < 2.2)	0.57 (0.33–1.15)	0.09.		
PLR (≥160 vs. < 160)	0.68 (0.54–0.88)	0.478		
Albumin (g/L) (≥35 vs. < 35)	0.79 (0.49–1.58)	0.692		
GFR (mL/min) (per unit)	1.12 (1.11–1.13)	0.021*		
Creatine kinase, U/L (≥185 vs. < 185)	0.62 (0.36–1.22)	0.152		
Creatine kinase isoenzymes MB, ng/mL (≥5 vs. < 5)	1.46 (0.81–2.88)	0.447		
Myoglobin, μg/L (≥100 vs. < 100)	0.21 (0.12–0.76)	1.65e-03**		
Lactate, mmol/L (≥1.7 vs. < 1.7)	0.77 (0.26–1.22)	0.194		
PF ratio, mmHg (≥300 vs. < 300)	1.75 (0.99–3.12)	0.0405*	1.45 (1.21–1.97)	0.04133*

ALT: alanine aminotransferase; AST: aspartate aminotransferase; NLR: neutrophil-to-lymphocyte ratio; PLR: platelet-to-lymphocyte ratio; GFR: glomerular filtration rate; PF ratio: PaO2/FiO2 ratio. Significance codes: "***"0.001, "**"0.01, "*"0.05, "."0.1, " "1.

severity [12]. Several days after COVID-19 infection, patients presented symptoms such as fever, coughing, sputum, vomiting, and diarrhea, and they were diagnosed and treated in the hospital. Fever (≥37.3°C) was an initial important event integral to immune response [13]; however, it was not significantly associated with LOS in univariate analysis.

Platelets are part of the first line of defense against lung-specific entry of SARS-CoV-2 [14], and among patients who had the lowest platelet counts, mortality decreased with an increase in platelet count [15]. The improvement in platelet count might have indicated clinical improvement. Monitoring of platelet counts is certainly beneficial to clinicians in

(a)

(b)

AUC: 0.886, 95% CI (0.819–0.954)
Brier score: 0.109, 95% CI (0.071–0.147)

Adjusted AUC: 0.860, 95% CI (0.727–0.954)
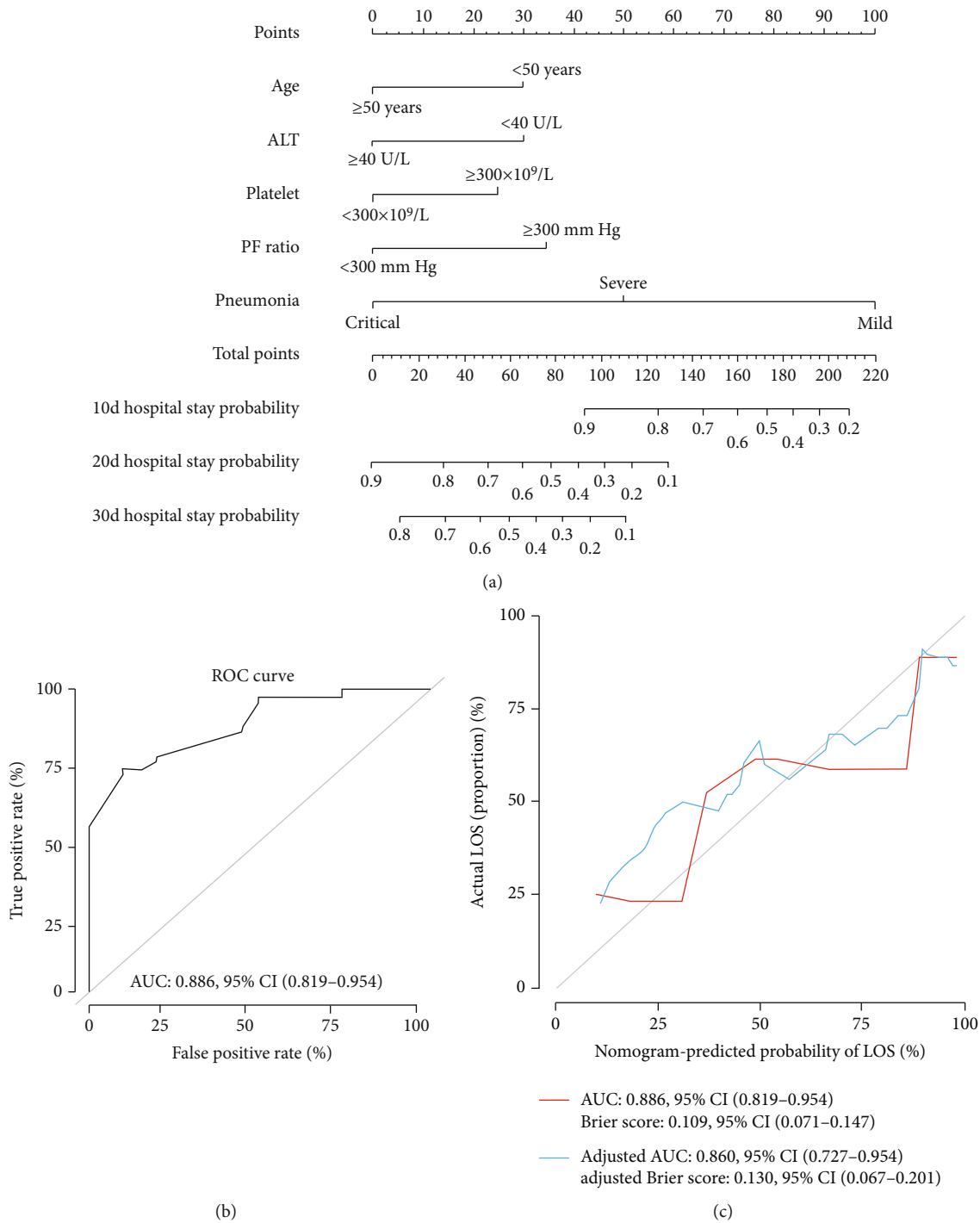adjusted Brier score: 0.130, 95% CI (0.067–0.201)

(c)

FIGURE 2: The nomogram and its predictive accuracy and discriminative ability. (a) Nomogram for the estimation of the probability of hospital stay of COVID-19 pneumonia patients. (b) Receiver operating characteristic curve of the nomogram. (c) The calibration curve showed favorable agreement between prediction by the nomogram and actual observations. The adjusted values were calculated by the bootstrap crossvalidation method, repeated 1000 times. ALT: alanine aminotransferase; PF ratio: PaO_2/FiO_2 ratio.

rare resource environments, where the chance of laboratory examination may be limited; however, the whole blood count may be relatively easy [15, 16].

Acute respiratory distress syndrome (ARDS), characterized by hypoxemia with a PaO_2/FiO_2 ratio (P/F ratio) ≤ 200 mmHg, is the primary cause of death due to COVID-19.

ARDS is a heterogeneous clinical syndrome, which is mechanically induced by uncontrolled COVID-19 viral replication and host cytokine storm. COVID-19 has unique ARDS characteristics in medical imaging and has been reported as a variable in several diagnostic studies. Artificial intelligence is a diagnostic tool that combines multiple
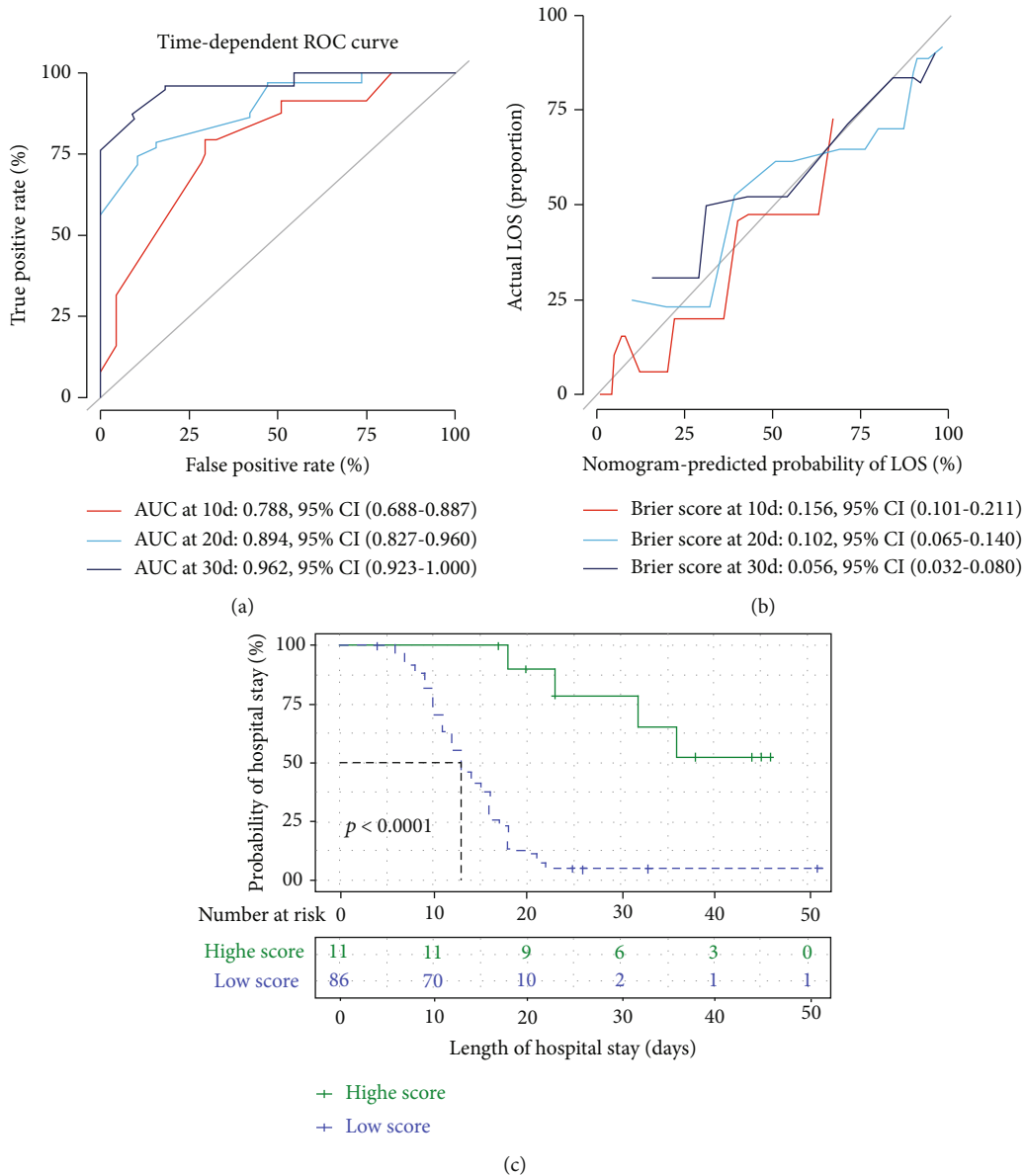
(a)

(b)

(c)

FIGURE 3: Time-dependent receiver operating characteristic curve showing area under curve (AUC) values at 10 (red), 20 (blue), and 30 (black) days (a). The Brier score of the calibration curve for the nomogram at 10 (red), 20 (blue), and 30 (black) days (b). Kaplan–Meier curves comparing the probability of hospital stay among the different patient groups, stratified by the fit score of the five-covariate nomogram model (c). p values were calculated using the log-rank test.

imaging modalities, including lung CT, chest radiography, and lung ultrasound [17]. Accordingly, AI assisted us to comprehensively interpret clinical and multiomics data of ARDS patients, and it is potentially advantageous in the management of ARDS patients in the future with individual treatment plans [18].

There are certain limitations to our study. First, this was a single-center, retrospective cohort study involving approximately a quarter of the COVID-19 patients in Beijing on March 21, 2020. This was not representative of the overall COVID-19 treatment or LOS in this area. Second, owing to low mortality (5/102), this study could not analyze the risk factors for survival. Third, due to the retrospective cohort

design, laboratory tests were not performed for all cytokines. For example, interferon-inducible protein-10 and IL-6 are predictive factors for SARS [19] and COVID-19 [7] outcomes, respectively; yet, they were excluded.

5. Conclusions

We successfully developed and validated a nomogram, which incorporated five independent predictors of LOS. Provided a future, large sample size cohort study that is used to validate the model, it may be useful in optimizing discharge strategies, hence shortening LOS in patients with COVID-19.

Data Availability

The data used to support the findings of this study are included within the article.

Conflicts of Interest

The authors declare that there is no conflict of interest regarding the publication of this paper.

References

[1] M. Liu, W. N. Liang, Q. Chen et al., "Risk factors for SARS-related deaths in 2003, Beijing," *Biomedical and Environmental Sciences: BES*, vol. 19, no. 5, pp. 336–339, 2006.

[2] C. M. Booth, L. M. Matukas, G. A. Tomlinson et al., "Clinical features and short-term outcomes of 144 patients with SARS in the greater Toronto area," *JAMA*, vol. 289, no. 21, pp. 2801–2809, 2003.

[3] A. Zumla, D. S. Hui, and S. Perlman, "Middle East respiratory syndrome," *The Lancet*, vol. 386, no. 9997, pp. 995–1007, 2015.

[4] World Health Organization, "Coronavirus disease 2019 (COVID-19) situation report situation report-62," March 2020, https://www.who.int/docs/default-source/coronaviruse/situation-reports/20200322-sitrep-62-covid-19.pdf?sfvrsn=755c76cd_2.

[5] Beijing Municipal Health Commission, "Update on the Novel Coronavirus Pneumonia Outbreak March 21, 2020," March 2020, http://wjw.beijing.gov.cn/wjwh/ztzl/xxgzbd/gzbdyqtb/202003/t20200322_1726678.html.

[6] Y. Hong, X. Wu, J. Qu, Y. Gao, H. Chen, and Z. Zhang, "Clinical characteristics of Coronavirus Disease 2019 and development of a prediction model for prolonged hospital length of stay," *Annals of translational medicine*, vol. 8, no. 7, 2020.

[7] F. Zhou, T. Yu, R. Du et al., "Clinical course and risk factors for mortality of adult inpatients with COVID-19 in Wuhan, China: a retrospective cohort study," *The Lancet*, vol. 395, no. 10229, pp. 1054–1062, 2020.

[8] K. W. Choi, T. N. Chau, O. Tsang et al., "Outcomes and prognostic factors in 267 patients with severe acute respiratory syndrome in Hong Kong," *Annals of Internal Medicine*, vol. 139, no. 9, pp. 715–723, 2003.

[9] K. H. Hong, J. P. Choi, S. H. Hong et al., "Predictors of mortality in middle east respiratory syndrome (MERS)," *Thorax*, vol. 73, no. 3, pp. 286–289, 2018.

[10] S. M. Opal, T. D. Girard, and E. W. Ely, "The immunopathogenesis of sepsis in elderly patients," *Clinical Infectious Diseases*, vol. 41, Supplement 7, pp. S504–S512, 2005.

[11] J. N. Pettiford, j. Jason, O. C. Nwanyanwu et al., "Age-related differences in cell-specific cytokine production by acutely ill Malawian patients," *Clinical and Experimental Immunology*, vol. 128, no. 1, pp. 110–117, 2002.

[12] M. L. DeDiego, J. L. Nieto-Torres, J. M. Jimenez-Guardeño et al., "Coronavirus virulence genes with main focus on SARS-CoV envelope gene," *Virus Research*, vol. 194, no. 19, pp. 124–137, 2014.

[13] T. Hampton, "Fever induces a molecular homing response in immune cells during infection," *JAMA*, vol. 321, no. 17, pp. 1657-1658, 2019.

[14] J. Thachil, "What do monitoring platelet counts in COVID-19 teach us?," *Journal of Thrombosis and Haemostasis*, vol. 18, no. 8, pp. 2071-2072, 2020.

[15] X. Yang, Q. Yang, Y. Wang et al., "Thrombocytopenia and its association with mortality in patients with COVID-19," *Journal of Thrombosis and Haemostasis*, vol. 18, no. 6, pp. 1469–1472, 2020.

[16] Y. Zheng, Y. Zhang, H. Chi et al., "The hemocyte counts as a potential biomarker for predicting disease progression in COVID-19: a retrospective study," *Clinical Chemistry and Laboratory Medicine*, vol. 58, no. 7, pp. 1106–1115, 2020.

[17] J. S. Suri, S. Agarwal, S. K. Gupta et al., "A narrative review on characterization of acute respiratory distress syndrome in COVID-19-infected lungs using artificial intelligence," *Computers in Biology and Medicine*, vol. 130, p. 104210, 2021.

[18] Z. Zhang, E. P. Navarese, B. Zheng et al., "Analytics with artificial intelligence to advance the treatment of acute respiratory distress syndrome," *Journal of Evidence-Based Medicine*, vol. 13, no. 4, pp. 301–312, 2020.

[19] N. L.-S. Tang, P. K.-S. Chan, C.-K. Wong et al., "Early enhanced expression of interferon-inducible protein-10 (CXCL-10) and other chemokines predicts adverse outcome in severe acute respiratory syndrome," *Clinical Chemistry*, vol. 51, no. 12, pp. 2333–2340, 2005.

Research Article

Prognostic Value of the Red Cell Distribution Width in Patients with Sepsis-Induced Acute Respiratory Distress Syndrome: A Retrospective Cohort Study

Huabin Wang,[1,2] Junbin Huang,[1,2] Wenhua Liao,[3] Jiannan Xu,[4] Zhongyuan He,[5] Yong Liu,[1,2] Zhijie He ,[3] and Chun Chen [1,2]

[1]*Division of Hematology/Oncology, Department of Pediatrics, The Seventh Affiliated Hospital of Sun Yat-Sen University, Shenzhen 518107, China*
[2]*Department of Pediatric Intensive Care Unit, The Seventh Affiliated Hospital of Sun Yat-Sen University, Shenzhen 518107, China*
[3]*Department of Intensive Care Unit, Sun Yat-Sen Memorial Hospital of Sun Yat-Sen University, Guangzhou 510000, China*
[4]*Center of Digestive Disease, The Seventh Affiliated Hospital of Sun Yat-Sen University, Shenzhen 518107, China*
[5]*Department of Orthopedics, The Seventh Affiliated Hospital of Sun Yat-Sen University, Shenzhen 518107, China*

Correspondence should be addressed to Zhijie He; hezhijie@mail.sysu.edu.cn and Chun Chen; chenchun69@126.com

Objective. The prognostic value of the red cell distribution width (RDW) in patients with sepsis-induced acute respiratory distress syndrome (ARDS) is still elusive. This study is aimed at determining whether RDW is a prognostic indicator of sepsis-induced ARDS. *Methods.* This retrospective cohort study included 1161 patients with sepsis-induced ARDS. The datasets were acquired from the Medical Information Mart for Intensive Care III database. The locally weighted scatter-plot smoothing technique, Cox regression, Kaplan-Meier estimator, and subgroup analysis were carried out to evaluate the association between RDW and 90-day mortality. *Results.* The RDW and mortality had a roughly linear increasing relationship. The Cox regression model results were as follows: for level 2 ($14.5\% < RDW < 16.2\%$), hazard ratio (HR) = 1.35, 95% confidence interval (CI) = $1.03 - 1.77$, and for level 3 ($RDW \geq 16.2\%$), HR = 2.07, 95% CI = $1.59 - 2.69$. The following results were obtained when RDW was treated as a continuous variable: HR = 1.11, 95%CI = $1.06 - 1.15$. The *P* values of the interaction between the RDW and covariates were greater than 0.05. *Conclusion.* RDW is a new independent prognostic marker for patients with sepsis-induced ARDS.

1. Introduction

Sepsis is caused by an imbalance in a host's response to infection and can lead to systemic multiple-organ dysfunction [1]. The lung is the first organ with the highest incidence rate of sepsis, and acute lung injury (ALI) is the main manifestation. ALI can further develop into acute respiratory distress syndrome (ARDS), an emergency and critical illness in the intensive care unit (ICU). It can cause excessive and uncontrolled inflammatory reactions [2], resulting in a clinical mortality rate (MR) as high as 35%–40% [3]. Therefore, early

discrimination of high-risk sepsis-induced ARDS patients with worse prognoses is extremely important.

The red cell distribution width (RDW) is commonly assessed as part of a complete blood count and is often used to identify different types of anemia. RDW has received much attention from the healthcare community as a new diagnostic and prognostic indicator in recent years. Several studies have shown a close association between RDW and the prognosis of burns [4], pancreatitis [5], peritonitis [6], hepatitis B-related diseases [7], cardiovascular diseases [8, 9], and cancer [10–13]. However, no study has reported on
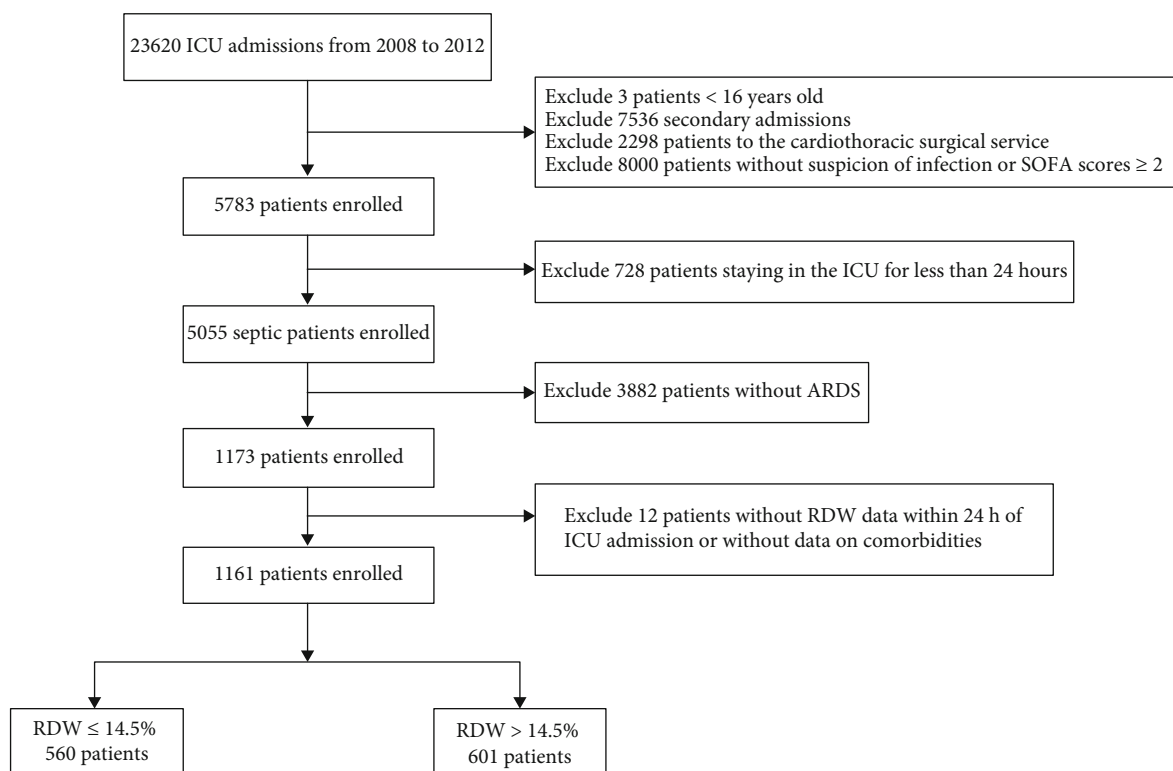
Figure 1: Flow diagram of patient recruitment.

the association between RDW and the prognosis of sepsis-induced ARDS patients. Moreover, clinical indicators for evaluating the prognosis of sepsis-induced ARDS patients are lacking. Therefore, this research is aimed at determining the predictive value of RDW in the MR of sepsis-induced ARDS patients.

2. Methods

2.1. Introduction to the Medical Database. The Medical Information Mart for Intensive Care III (MIMIC-III) V.1.4 database is a freely accessible critical care database that contains the clinical data of at least forty thousand critically ill patients hospitalized at the Beth Israel Deaconess Medical Center of Harvard Medical School between 2001 and 2012 (58,976 inpatients in total) [14]. The MIMIC-III database consists of comprehensive patient data such as biochemical, demographic, and physiological data as well as clinical diagnostics and medical treatment records. The MIMIC-III database not only has a large sample size and rich data types but also high-quality and high-reliability data. It is a treasure chest for clinical research in the field of critical care medicine. Wang obtained access to the database and was involved in data extraction (Certification No. 36132199).

2.2. Selection Criteria. We focused on the patients who were admitted to the ICUs from 2008 to 2012. All patients were required to meet the diagnostic criteria for ARDS and sepsis within 24 h of admission to the ICU. According to the recommendations of the Surviving Sepsis Campaign in 2016 [15]

and the extraction method for sepsis-3 patients described by Johnson and coworkers [16], this study included patients suspected of having an infection during ICU admission (within 24 h) with a Sequential Organ Failure Assessment (SOFA) score of ≥2. Clinically suspected infection was diagnosed by bacterial culture positivity and antibiotic administration. According to the Berlin diagnostic criteria of ALI/ARDS, ARDS was defined by the following parameters: (i) mechanical ventilation and positive end-expiratory pressure or continuous positive airway pressure ≥ 5 cmH$_2$O; (ii) severe (PaO$_2$/FiO$_2$ ≤ 100 mmHg), moderate (PaO$_2$/FiO$_2$ = 100 – 200 mmHg), or mild (PaO$_2$/FiO$_2$ = 200 – 300 mmHg); and (iii) without pleural effusion, lung collapse, lung nodules, or cardiogenic pulmonary edema. Since no cardiogenic pulmonary edema information was available directly from the database, the patients with a pulmonary capillary wedge pressure (PCWP) of ≥18 cmH$_2$O were considered to have cardiogenic pulmonary edema.

Patients with the following criteria were excluded: (i) younger than sixteen years, (ii) admitted to the ICU before, (iii) admitted to the cardiothoracic surgery service, (iv) stayed in the ICU for <24 h, (v) suspected with infection > 24 h before and after ICU admission, and (vi) no RDW data available within 24 h of ICU admission or no data on comorbidities.

2.3. Data Extraction and Patient Outcomes. The demographic characteristics (e.g., age, sex, and ethnicity), comorbidities (congestive heart failure, anemia, hypertension, chronic respiratory disease, liver disease, and kidney failure)

TABLE 1: Baseline data of the study subjects.

Variable	Total ($n = 1161$)	RDW ≤ 14.5% ($n = 560$)	RDW > 14.5% ($n = 601$)	P value
Age, year	64.2 ± 17.3	63.3 ± 17.9	65.0 ± 16.8	0.098
Male, n (%)	660 (56.8%)	340 (60.7)	320 (53.3)	0.010
Ethnicity, n (%)				0.749
White	811 (69.9)	394 (70.4)	417 (69.4)	
Black	85 (7.3)	43 (7.7)	42 (7.0)	
Other	265 (22.8)	123 (22.0)	142 (23.6)	
SOFA, median (IQR)	7 (4–10)	6 (4–9)	5 (7–11)	<0.001
ARDS stage, n (%)				0.018
Mild	326 (28.1)	148 (26.4)	178 (29.6)	
Moderate	517 (44.5)	273 (48.8)	244 (40.6)	
Severe	318 (27.4)	139 (24.8)	179 (29.8)	
Vasopressin use, n (%)	609 (52.5)	269 (48.0)	340 (56.6)	0.004
Comorbidities, n (%)				
Congestive heart failure	242 (20.8)	98 (17.5)	144 (24.0)	0.007
Chronic pulmonary	291 (25.1)	126 (22.5)	165 (27.5)	0.052
Hypertension	174 (15.0)	55 (9.8)	119 (19.8)	<0.001
Renal failure	198 (17.1)	61 (10.9)	137 (22.8)	<0.001
Liver disease	118 (10.2)	28 (5.0)	90 (15.0)	<0.001
Anemia	299 (25.8)	121 (21.6)	178 (29.6)	0.002
Laboratory data				
White blood cell, 10^9/L	10.6 (7.6–14.3)	10.9 (8.2–14.3)	10 (6.9–14.3)	0.006
Platelet, 10^9/L	202 (147–271)	212 (167–278)	186 (125–264)	<0.001
Glucose, mg/dL	133 (107–175)	136 (110–178)	129 (104–173)	0.003
Creatinine, mg/dL	1.1 (0.8–1.7)	1.0 (0.8–1.5)	1.2 (0.8–2.1)	<0.001
Urea nitrogen, mg/dL	22 (15–37)	19.5 (13.0–29.0)	26 (17–44)	<0.001
Clinical outcome				
30-day mortality, n (%)	318 (27.4)	104 (18.6)	214 (35.6)	<0.001
90-day mortality, n (%)	379 (32.6)	122 (21.8)	257 (42.8)	<0.001

and laboratory data (RDW, platelet count, white blood cell count, blood glucose, urea nitrogen, and serum creatinine), and severity of the disease (SOFA score, ARDS grade, and vasopressin use) of the included patients were extracted from the database. All laboratory parameters were selected for the first measurement. The outcome measure was all-cause MR during the 90 days of ICU admission.

2.4. Grouping. Since none of the patients had an RDW less than the normal range (11.5%–14.5%), the patients were categorized into the normal RDW (nRDW) group (RDW ≤ 14.5%) and the increased RDW (iRDW) group (RDW > 14.5%). Locally weighted scatter-plot smoothing (LOWESS) analysis revealed approximately linearly increasing relationship between the RDW and 90- or 30-day all-cause mortalities. Therefore, the iRDW group was subdivided into 2 subgroups using the median value of the RDW as the threshold and then inputting it into the Cox regression model to further explore the impact of an increased RDW on mortality. The resulting three groups were level 1 (RDW ≤ 14.5%), level 2 (14.5% < RDW < 16.2%), and level 3 (RDW ≥ 16.2%).

2.5. Treatment of Missing Values. The missing values were <5% for all the variables included in the present study. The normally distributed variables were subjected to mean imputation, while the nonnormally distributed variables were subjected to median imputation. For the categorical variables with missing values, the associated cases were deleted directly.

2.6. Statistical Analysis. Categorical variables were analyzed by the chi-square test, and the data are expressed as percentages. Continuous variables were tested with Student's t test (normal distribution) or the Mann-Whitney U test, and the results are presented as the mean ± standard deviation or median (interquartile range (IQR)). The LOWESS method was employed to assess the general association between RDW and 90- or 30-day all-cause mortalities. The Kaplan-Meier estimator was applied to construct the survival curves of different RDWs, which were compared with the log-rank test. Then, Cox regression was employed to analyze the prognostic factors related to mortality. The variables with $P <$ 0.05 in the univariate model were subjected to multivariate Cox regression analysis. Covariate correction was performed
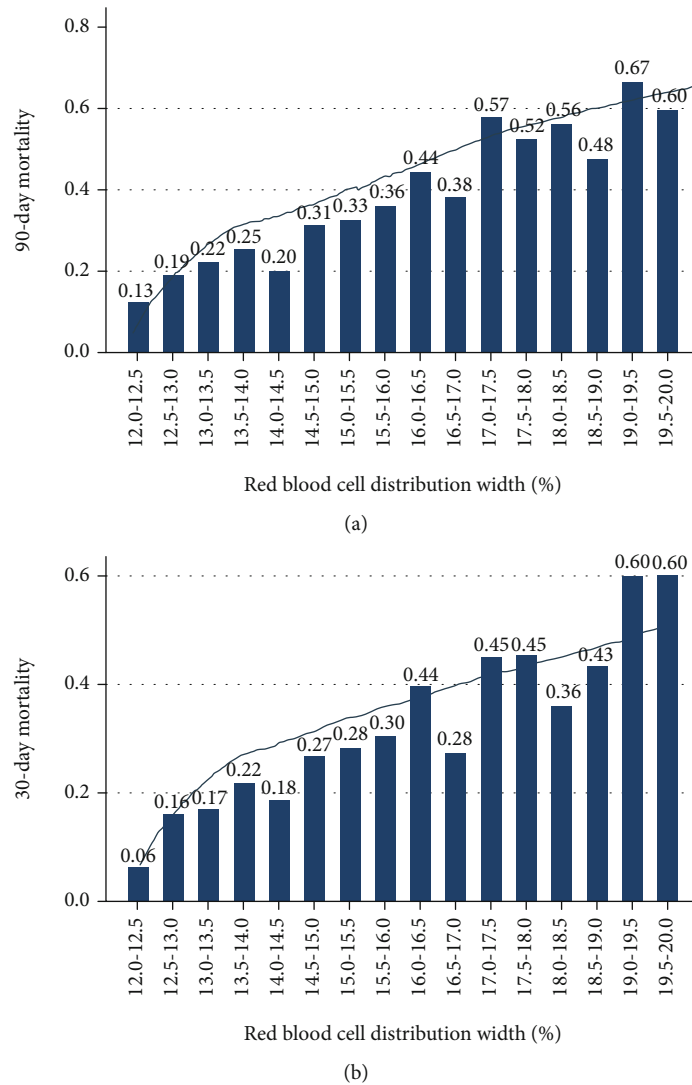
(a)

(b)

FIGURE 2: Relationship between RDW and (a) 90-day or (b) 30-day mortality in sepsis-induced ARDS.

using the following models: Model 1 was corrected according to age, sex, and ethnicity; Model 2 = Model 1 + (ARDS grade, comorbidities, and vasopressin use); Model 3 = Model 2 + (RDW, platelet count, and white blood cell count as well as levels of blood sugar, urea nitrogen, and serum creatinine); and Model 4 = Model 3 + (the SOFA scores). Multicollinearity was examined by the variance-inflation factor (VIF), and VIF ≥ 10 (severe multicollinearity) was not allowed in the study.

In the Cox regression model, subgroup analysis was performed according to the severity of illness during ICU admission [17], including the ARDS grade and in combination with septic shock. However, identifying septic shock patients in the aforementioned datasets was difficult because of the lack of access to relevant information. Therefore, it was substituted with vasopressin use within 24 h of ICU admission. Considering that RDW could be affected by the hemoglobin level, another subgroup analysis was carried out according to the association of RDW with anemia. To verify the interaction between the RDW and these variables, the

regression model was incorporated with multiplicative interaction terms. The significance level was set at P value < 0.05. All statistical tests were conducted with Stata v.16, SPSS v.24, and R v.3.6.3.

3. Results

3.1. Baseline Characteristics. A total of 1161 patients with sepsis-induced ARDS were included in this analysis. The patient selection and data screening processes are illustrated in Figure 1. The overall 90-day all-cause MR was 32.6%. The baseline characteristics of the nRDW and iRDW groups were compared and are presented in Table 1. The overall mean age at ICU admission was 64.2 years, and 56.8% of the patients were male. The frequency of vasopressin use in the iRDW group was remarkably higher than that in the nRDW group (56.6% vs. 48.0%, $P = 0.004$). Moreover, the iRDW group showed a higher proportion of comorbidities, such as congestive heart failure, anemia, high blood pressure, liver disease, and kidney failure. The 90-day MR in the iRDW
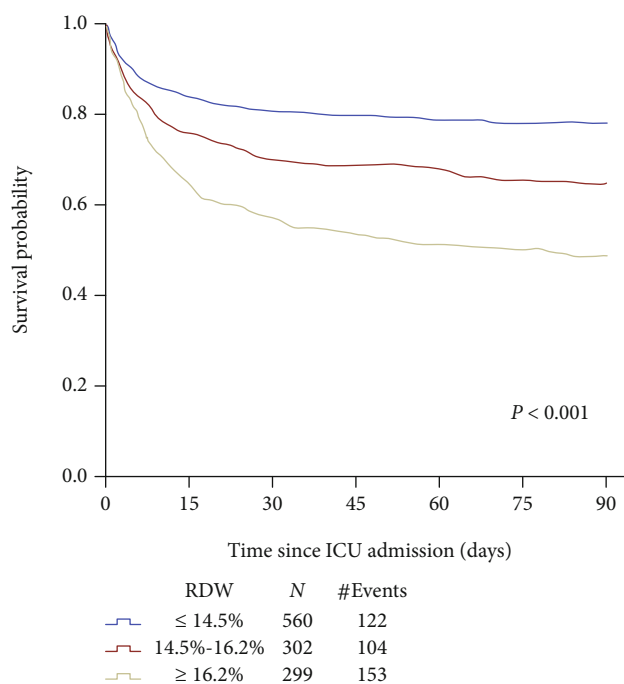
FIGURE 3: Association between RDW and 90-day overall survival in sepsis-induced ARDS.

TABLE 2: HR values for the 90-day MR among the 3 RDWs.

| | RDW ≤ 14.5% | | 14.5% < RDW < 16.2% | | RDW ≥ 16.2% | |
	HR (95% CI)	P	HR (95% CI)	P	HR (95% CI)	P
Model 1	Reference	—	1.61 (1.24–2.10)	<0.001	2.68 (2.11–3.40)	<0.001
Model 2	Reference	—	1.50 (1.15–1.95)	0.003	2.35 (1.83–3.01)	<0.001
Model 3	Reference	—	1.45 (1.11–1.90)	0.006	2.14 (1.65–2.78)	<0.001
Model 4	Reference	—	1.35 (1.03–1.77)	0.028	2.07 (1.59–2.69)	<0.001

group was remarkably higher than that in the nRDW group (42.8% vs. 21.8%, $P < 0.001$).

3.2. Relationship between RDW and Mortality.
An approximately increasing linear relationship was found between RDW and mortality using the LOWESS technique (Figure 2). When the RDW was in the range of 19.0%–19.5%, the 90-day mortality rate was as high as 67%, and the 30-day MR was 60%. Figure 3 represents the Kaplan-Meier curve describing the association between RDW and 90-day MR in different RDW groups. For various time periods, the level 1 group showed the highest survival rate ($P < 0.001$), followed by the level 2 group.

In the extended multivariate Cox regression model, the level 3 RDW was significantly correlated with the 90-day MR (Table 2). Model 1 showed a hazard ratio (HR) of 2.68 with a 95% confidence interval (CI) of 2.11–3.40. Model 2 had an HR of 2.35 with a 95% CI of 1.83–3.01. Model 3 exhibited an HR of 2.14 with a 95% CI of 1.65–2.78. Model 4 had an HR of 2.07 with a 95% CI of 1.59–2.69. Level 2 exhibited similar results with smaller HR values. Supplementary Table 1 lists the HR values of all covariates in Model 4.

TABLE 3: HR values for the 90-day MR with RDW as a continuous variable.

| | RDW as a continuous variable (per 1% increase) | |
	HR (95% CI)	P
Model 1	1.16 (1.47-2.23)	<0.001
Model 2	1.13 (1.09-1.17)	<0.001
Model 3	1.11 (1.07-1.16)	<0.001
Model 4	1.11 (1.06-1.15)	<0.001

When RDW was regarded as a continuous variable, it could also predict 90-day MR (HR, 1.11 per 1% increase; 95% CI, 1.06–1.15) (Table 3).

3.3. Subgroup Analysis.
The results of the subgroup analysis are shown in Figure 4. The P values of the interaction between RDW and the degree of ARDS, use of vasopressors, and anemia were 0.241, 0.719, and 0.911, respectively. There were no obvious differences between the RDW and mortality among patients with different degrees of ARDS, whether vasopressin was used and whether anemia was present.
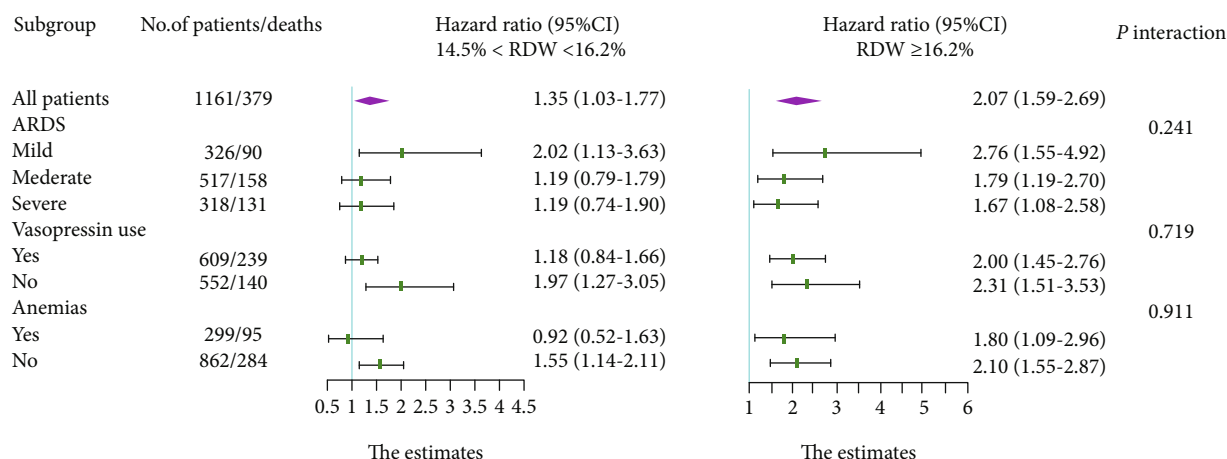
Subgroup	No.of patients/deaths	Hazard ratio (95%CI) 14.5% < RDW <16.2%	Hazard ratio (95%CI) RDW ≥16.2%	P interaction
All patients	1161/379	1.35 (1.03-1.77)	2.07 (1.59-2.69)	
ARDS				0.241
Mild	326/90	2.02 (1.13-3.63)	2.76 (1.55-4.92)	
Moderate	517/158	1.19 (0.79-1.79)	1.79 (1.19-2.70)	
Severe	318/131	1.19 (0.74-1.90)	1.67 (1.08-2.58)	
Vasopressin use				0.719
Yes	609/239	1.18 (0.84-1.66)	2.00 (1.45-2.76)	
No	552/140	1.97 (1.27-3.05)	2.31 (1.51-3.53)	
Anemias				0.911
Yes	299/95	0.92 (0.52-1.63)	1.80 (1.09-2.96)	
No	862/284	1.55 (1.14-2.11)	2.10 (1.55-2.87)	

Figure 4: Adjusted hazard ratio in the subgroup analysis.

4. Discussion

In this study, massive amounts of data were obtained from the MIMIC-III database to assess the prognostic significance of RDW in sepsis-induced ARDS patients. The results demonstrated that RDW and mortality had a roughly linear increasing relationship. Multivariate Cox regression analysis indicated that RDW was independently associated with the high MR of sepsis-induced ARDS patients.

Our results were in good agreement with previous findings that RDW demonstrated good predictive value for many diseases, especially inflammatory diseases. In a retrospective study of 610 patients with severe burns, RDW independently correlated with the occurrence of ARDS. For every 1% increase in RDW, the risk of ARDS was induced by 29% [18]. Ganji et al. conducted a meta-analysis involving 7 studies with 976 patients with pancreatitis. They used the summary receiver operating characteristic (ROC) curve from a bivariate model to predict the prognosis of RDW for patient mortality and obtained an area under the curve (AUC) of 0.757 as well as pooled specificity and sensitivity of 90% (95% CI: 73%–96%) and 67% (95% CI: 51%–80%), respectively [19]. Interestingly, RDW might also be related to the risk of death in the general population. In a study involving 15,852 adults living in the community, the researchers followed up the community residents for 6–12 years and found that the mortality increased twofold from the lowest quintile of the RDW to the highest quintile [20]. Moreover, RDW was also involved in the occurrence of cancers (HR, 1.28; 95% CI, 1.21–1.36), cardiovascular diseases (HR, 1.22; 95% CI, 1.14–1.31), and chronic respiratory diseases (HR, 1.32; 95% CI, 1.17–1.49) [20].

The correlation mechanism between increased RDW and poor prognosis in patients with sepsis-induced ARDS remains elusive. Sepsis-induced ARDS is a systemic inflammatory response syndrome [21]. To date, the link between the inflammatory response and the increase in RDW has been confirmed. Studies have shown a positive correlation between RDW and certain inflammatory biomarkers (erythrocyte sedimentation rate and C-reactive protein) [22, 23],

indicating that red blood cell heterogeneity implies the existence of inflammation. Inflammation has adverse effects on bone marrow function, iron metabolism, and red blood cell homeostasis, further leading to the production of a large number of new reticulocytes related to RDW increase [24, 25]. In addition, the increase in oxidative stress boosted RDW by reducing the survival rate of red blood cells and releasing large numbers of premature red blood cells into the circulation [26]. These possible mechanisms might also explain the interaction between RDW and disease severity to a certain extent because the more severe the sepsis-induced ARDS is, the more remarkable the inflammatory response and oxidative stress.

One of the strengths of this research was the large study population, which was sufficient for further stratification and subgroup analysis of RDW. Furthermore, adequate confounding factors were included that might interact with RDW to produce more accurate results because RDW might be affected by a series of factors [27], such as age, sex, anemia, and liver and kidney dysfunction. Nevertheless, this research had some limitations. First, it was not a multicenter retrospective study and hence could have selection bias. Second, only the RDW data within 24 h of ICU admission were analyzed. Thus, follow-up data could be used to verify the findings of this study. Third, identifying patients with septic shock and cardiogenic edema in the datasets was difficult because of the lack of assessments of relevant information; they were replaced with vasopressin use and PCWP value. Last, the MIMIC-III V.1.4 database only included inpatients from 2001 to 2012 but did not include patients from more recent years.

5. Conclusion

In summary, this study suggested that RDW is a promising independent prognostic marker of sepsis-induced ARDS and that increased RDW is significantly correlated with poor prognosis. This study provided support for the risk stratification of patients with sepsis-induced ARDS based on RDWs. However, further multicenter prospective research

is required to assess the exact mechanism underlying the correlation between RDW and MR and hence further verify the findings.

Data Availability

Conflicts of Interest

The authors declare that there are no conflicts of interest.

Authors' Contributions

Huabin Wang and Junbin Huang contributed equally to this work.

Acknowledgments

Supplementary Materials

Supplementary Table 1: Cox proportional hazards model of factors associated with 90-day mortality among sepsis-induced acute respiratory distress syndrome. (*Supplementary Materials*)

References

[1] W. Schulte, J. Bernhagen, and R. Bucala, "Cytokines in Sepsis: Potent Immunoregulators and Potential Therapeutic Targets—An Updated View," *Mediators of Inflammation*, vol. 2013, Article ID 165974, 16 pages, 2013.

[2] D. C. Angus and T. van der Poll, "Severe sepsis and septic shock," *The New England Journal of Medicine*, vol. 369, no. 9, pp. 840–851, 2013.

[3] G. Bellani, J. G. Laffey, T. Pham et al., "Epidemiology, patterns of care, and mortality for patients with acute respiratory distress syndrome in intensive care units in 50 countries," *JAMA*, vol. 315, no. 8, pp. 788–800, 2016.

[4] L. Qiu, C. Chen, S. J. Li et al., "Prognostic values of red blood cell distribution width, platelet count, and red cell distribution width-to-platelet ratio for severe burn injury," *Scientific Reports*, vol. 7, no. 1, p. 13720, 2017.

[5] E. M. Yilmaz and A. Kandemir, "Significance of red blood cell distribution width and C-reactive protein/albumin levels in predicting prognosis of acute pancreatitis," *Ulusal Travma ve Acil Cerrahi Dergisi*, vol. 24, no. 6, pp. 528–531, 2018.

[6] P. He, J. P. Hu, H. Li et al., "Red blood cell distribution width and peritoneal dialysis-associated peritonitis prognosis," *Renal Failure*, vol. 42, no. 1, pp. 613–621, 2020.

[7] J. Wang, R. Huang, X. Yan et al., "Red blood cell distribution width: a promising index for evaluating the severity and long-term prognosis of hepatitis B virus-related diseases," *Digestive and Liver Disease*, vol. 52, no. 4, pp. 440–446, 2020.

[8] A. M. Adam, M. A. Ali, A. A. Shah et al., "Efficacy of hematological and coagulation parameters in the diagnosis and prognosis of patients with acute coronary syndrome," *The Journal of Tehran Heart Center*, vol. 13, no. 3, pp. 115–125, 2018.

[9] P. O. Guimarães, J. L. Sun, K. Kragholm et al., "Association of standard clinical and laboratory variables with red blood cell distribution width," *American Heart Journal*, vol. 174, pp. 22–28, 2016.

[10] B. Li, Z. You, X. Z. Xiong et al., "Elevated red blood cell distribution width predicts poor prognosis in hilar cholangiocarcinoma," *Oncotarget*, vol. 8, no. 65, pp. 109468–109477, 2017.

[11] W. Ge, J. Xie, and L. Chang, "Elevated red blood cell distribution width predicts poor prognosis in patients with oral squamous cell carcinoma," *Cancer Management and Research*, vol. 10, pp. 3611–3618, 2018.

[12] Y. Koma, A. Onishi, H. Matsuoka et al., "Increased red blood cell distribution width associates with cancer stage and prognosis in patients with lung cancer," *PLoS One*, vol. 8, no. 11, article e80240, 2013.

[13] D. Yao, Z. Wang, H. Cai, Y. Li, and B. Li, "Relationship between red cell distribution width and prognosis in patients with breast cancer after operation: a retrospective cohort study," *Bioscience Reports*, vol. 39, no. 7, 2019.

[14] A. E. Johnson, T. J. Pollard, L. Shen et al., "MIMIC-III, a freely accessible critical care database," *Scientific Data*, vol. 3, no. 1, article 160035, 2016.

[15] M. Singer, C. S. Deutschman, C. W. Seymour et al., "The third international consensus definitions for sepsis and septic shock (sepsis-3)," *JAMA*, vol. 315, no. 8, pp. 801–810, 2016.

[16] A. E. W. Johnson, J. Aboab, J. D. Raffa et al., "A comparative analysis of sepsis identification methods in an electronic database," *Critical Care Medicine*, vol. 46, no. 4, pp. 494–499, 2018.

[17] Y. Shen, X. Huang, and W. Zhang, "Platelet-to-lymphocyte ratio as a prognostic predictor of mortality for sepsis: interaction effect with disease severity-a retrospective study," *BMJ Open*, vol. 9, no. 1, article e022896, 2019.

[18] C. H. Xiao, J. Wan, H. Liu et al., "Red blood cell distribution width is an independent risk factor in the prediction of acute respiratory distress syndrome after severe burns," *Burns*, vol. 45, no. 5, pp. 1158–1163, 2019.

[19] A. Ganji, A. Esmaeilzadeh, O. Ghanaei et al., "Predictive value of red blood cell distribution width for mortality in patients with acute pancreatitis: a systematic review and meta-analysis," *Medical Journal of the Islamic Republic of Iran*, vol. 31, no. 1, pp. 823–828, 2017.

[20] T. S. Perlstein, J. Weuve, M. A. Pfeffer, and J. A. Beckman, "Red blood cell distribution width and mortality risk in a community-based prospective cohort," *Archives of Internal Medicine*, vol. 169, no. 6, pp. 588–594, 2009.

[21] J. A. Silversides, A. J. Ferguson, D. F. McAuley, B. Blackwood, J. C. Marshall, and E. Fan, "Fluid strategies and outcomes in patients with acute respiratory distress syndrome, systemic inflammatory response syndrome and sepsis: a protocol for a systematic review and meta-analysis," *Systematic Reviews*, vol. 4, no. 1, p. 162, 2015.

[22] A. Vayá, A. Sarnago, O. Fuster, R. Alis, and M. Romagnoli, "Influence of inflammatory and lipidic parameters on red blood cell distribution width in a healthy population," *Clinical Hemorheology and Microcirculation*, vol. 59, no. 4, pp. 379–385, 2015.

[23] G. Lippi, G. Targher, M. Montagnana, G. L. Salvagno, G. Zoppini, and G. C. Guidi, "Relation between red blood cell distribution width and inflammatory biomarkers in a large cohort of unselected outpatients," *Archives of Pathology & Laboratory Medicine*, vol. 133, no. 4, pp. 628–632, 2009.

[24] P. G. Fraenkel, "Anemia of inflammation: a review," *The Medical Clinics of North America*, vol. 101, no. 2, pp. 285–296, 2017.

[25] K. Bujak, J. Wasilewski, T. Osadnik et al., "The prognostic role of red blood cell distribution width in coronary artery disease: a review of the pathophysiology," *Disease Markers*, vol. 2015, Article ID 824624, 12 pages, 2015.

[26] B. Wang, Y. Gong, B. Ying, and B. Cheng, "Relation between red cell distribution width and mortality in critically ill patients with acute respiratory distress syndrome," *BioMed Research International*, vol. 2019, Article ID 1942078, 8 pages, 2019.

[27] Y. Chen and X. Li, "Can red blood cell distribution width predict the severity and prognosis of hepatitis B virus-related diseases?," *Digestive and Liver Disease*, vol. 52, no. 11, p. 1372, 2020.